Advanced Multidisciplinary Engineering Journal
AMEJ
ISSN: 3070-5797/© 2026 The Authors. (CC BY 4.0) License.
Journal Homepage
https://pub.scientificirg.com/index.php/AMEJ

Experimental validation and techno-economic assessment of façade-applied photovoltaics for nearly zero-energy building conversion in a Mediterranean climate: A Case Study of the Faculty of Engineering, Damanhur University

Abd Elrahman M. Mostafa Mohamed[a][1], Aly M. Elharidi[a], Nour A. Moharram[a], Mohamed M. Khairat Dawood[b]
[a] *Mechanical Engineering Department, College of Engineering and Technology, Arab Academy for Science, Technology and Maritime Transport, Alexandria, Egypt. Emails: Abdrhmanelkordy@gmail.com, alyelharidi@aast.edu.eg, nourmoharram@aast.edu.eg,*
[b] *Mechanical Power Engineering, Faculty of Engineering, Damanhur University, Elbehira, Egypt. Email: mohamed.dawood@eng.dmu.edu.eg*

ABSTRACT
This study develops an experimentally supported framework for assessing façade-applied photovoltaic (PV) systems as a strategy for reducing grid-electricity demand and evaluating building energy performance in a Mediterranean educational building. The Faculty of Engineering, Damanhour University, Egypt, is considered as the sole case study. The methodology integrates localized field electrical testing, a weather-adjusted July–August electrical time series, façade-specific annual solar-radiation screening, controlled DesignBuilder/EnergyPlus simulations, and a transparent module-cost economic assessment. A field test conducted on 2 July 2026 recorded a mean current of 2.72 A and peak current of 3.57 A, corresponding to mean and peak power outputs of 41.42 and 54.33 W for the conventional PV test. A separate two-point BIPV test recorded a mean current of 8.05 A and mean power of 89.79 W. The weather-adjusted dataset covers 1 July–12 August 2026 at 30-minute intervals for JSM-195SP and JS-190W-Special modules installed at 90° and 30°. Annual solar-radiation screening identified Elevation 1 as the most favorable vertical façade, receiving 1,141.2 kWh/m²·year, while the roof received 1,726.8 kWh/m²·year. The annual building assessment uses 8,760-hour DesignBuilder/EnergyPlus simulations with a common modeled PV façade allocation of 1,123.20 m². A baseline and four PV scenarios were evaluated. JSM-195SP at 30° generated 229,119.60 kWh/year and reduced net grid electricity consumption by 217,663.62 kWh/year (18.93%), reducing Net EUI to 200.70 kWh/m²·year and simulated district cooling by 7.41%. Based on an electricity tariff of 1.95 EGP/kWh and module prices of 6,000 EGP/panel for JSM-195SP and 12,000 EGP/panel for JS-190W-Special, simple module-cost payback periods were 13.03, 100.55, 6.20, and 46.24 years for JSM-195SP at 90°, JS-190W-Special at 90°, JSM-195SP at 30°, and JS-190W-Special at 30°, respectively. Using the 2026 EIB Egypt intermittent-generation factor of 0.498 kgCO₂/kWh, annual avoided operational emissions were estimated at 51.63, 32.20, 108.40, and 70.02 tCO₂/year, respectively. These represent emission reductions and potential carbon-credit quantities subject to applicable certification and additionality requirements. The study does not claim calibrated annual utility validation or whole-building net-zero status; rather, it establishes a reproducible evidence chain linking measured electrical behavior, façade selection, annual simulation, environmental assessment, and investment screening.

PAPER INFORMATION

HISTORY
Received: 15 August 2026
Revised: 20 September 2026
Accepted: 25 October 2026
Online: 29 October 2026

MSC
76M10, 86A10, 90B50

KEYWORDS
façade-applied photovoltaics; Building-integrated photovoltaics; Nearly zero-energy buildings; Solar-radiation screening; Techno-economic assessment.

[1] *Mechanical Engineering Department, College of Engineering and Technology, Arab Academy for Science, Technology and Maritime Transport, Alexandria, Egypt. Email: Abdrhmanelkordy@gmail.com*

1. INTRODUCTION

The decarbonization of buildings and energy-intensive facilities has become an essential priority within the global transition toward low-carbon energy systems [1,2]. Administrative, institutional, educational, and service buildings can represent a persistent energy burden because they combine extended operating hours, dense electrical equipment, continuous lighting, and substantial cooling demand. Improving building energy performance is therefore an important component of operational cost reduction, energy resilience, and long-term decarbonization planning [5,6].

Within this context, nearly zero-energy buildings (NZEBs) have emerged as a practical pathway for reducing dependence on conventional grid electricity. The NZEB concept requires a clear accounting boundary and a transparent distinction between demand reduction and renewable-energy supply [7,35]. For institutional buildings, the daily occupancy profile, cooling requirements, and equipment loads can coincide with periods of high solar availability, creating a favorable technical basis for photovoltaic integration [8].

Building-integrated photovoltaics provide an architecturally integrated alternative to conventional building-applied photovoltaic systems [9,10]. However, the present study deliberately uses the more precise term façade-applied PV for the investigated opaque modules. The tested Jet Solar modules are conventional opaque crystalline-silicon PV products mounted on façade collector surfaces; they are not semi-transparent photovoltaic glazing, and no glazing-specific optical properties are assumed. This terminology avoids conflating opaque façade-mounted PV with genuine photovoltaic glazing, while retaining the broader BIPV context where the PV layer is intended to function as part of the building envelope.

The importance of façade PV becomes particularly evident in Mediterranean climates, where strong solar resources coexist with significant cooling demand. Elevated temperatures can reduce PV conversion efficiency through thermal derating [12], while local obstructions, neighboring buildings, parapets, service structures, and other site elements can generate highly non-uniform shading [13,42]. Consequently, manufacturer-rated power under standard test conditions is insufficient for deciding where and how façade PV should be deployed. Building-specific solar-access analysis and dynamic whole-building simulation are needed to connect façade geometry with electrical generation and building-energy effects.

Previous studies have demonstrated the importance of orientation, envelope properties, retrofit measures, and PV capacity in NZEB performance [15–25]. Nevertheless, the literature still benefits from studies that explicitly connect four levels of evidence within one controlled case: localized electrical measurements, façade-specific solar-resource assessment, dynamic building simulation, and transparent lifecycle economics. The present study addresses this methodological gap using the Faculty of Engineering, Damanhour University, as the sole case study by comparing two PV module options under both the original vertical condition and a 30° inclined configuration.

The contribution of this study is not the isolated evaluation of façade photovoltaics or the use of building-energy simulation alone. Rather, it is the structured connection of four distinct evidence layers within a single existing educational-building case: short-duration field measurements of electrical behavior, façade-specific annual solar-radiation screening, controlled annual DesignBuilder/EnergyPlus scenarios, and economic screening based on simulated electricity performance. The study also distinguishes the whole-building grid-electricity reduction from the separate end-use electricity reference used for practical panel sizing. This distinction provides a transparent basis for interpreting both building-scale performance and the limitations of the proposed PV allocation. The resulting framework is intended as a reproducible assessment procedure, not as proof of annual model calibration or achievement of net-zero energy status.

The study has five objectives: (1) characterize the measured daylight current–power response of the façade PV test; (2) identify the most favorable vertical surface through annual solar-radiation screening; (3) quantify module-type and inclination effects using controlled 8,760-hour DesignBuilder/EnergyPlus simulations; (4) assess building-energy, thermal, electrical, and environmental performance; and (5) evaluate grid-energy savings, simple payback, IRR, NPV, discounted payback, and levelized electricity cost under stated screening assumptions.

Five hypotheses guide the study: H1, localized electrical measurements reproduce the expected time-dependent current–power response; H2, inclination materially affects plane-of-array irradiance and electrical output; H3, PV integration reduces building energy demand and grid dependence versus baseline; H4, façade solar exposure and shading materially influence practical PV value; and H5, the preferred configuration balances electrical performance with acceptable lifecycle investment recovery, rather than minimizing gross total-site energy alone.

2. Case study: Faculty of Engineering, Damanhour University Study workflow and evidence hierarchy

The study followed a sequential evidence-based workflow shown in **Table 1**. Field tests measured current and electrical power under actual site conditions. Annual DesignBuilder/EnergyPlus simulations then assessed two PV modules at 90° and 30° inclinations. Defined module counts enabled normalization of annual generation to derive per-panel production and equivalent average power. These results determined the practical module count needed to offset 100% of the adopted annual Building Electricity reference. The sized configurations were assessed for façade-area requirements and module-cost payback, alongside annual building-energy, thermal, and carbon performance. This workflow distinguishes measurements, simulations, panel-level normalization, and sizing calculations within a reproducible methodology.

Table 1. Study workflow

Step	Method	Purpose/output
1	Field test	Direct experimental evidence of current and power behavior under actual site conditions.
2	Controlled annual DesignBuilder/EnergyPlus simulation	Annual PV generation for the four module–inclination configurations using a defined modeled panel count.
3	Panel-productivity normalization	Annual PV generation ÷ modeled panel count → kWh/panel·year and equivalent average power per panel.
4	100% Building Electricity sizing and economic interpretation	Annual Building Electricity reference ÷ panel productivity → practical panel count; then façade-area requirement and module-cost payback.

The Faculty of Engineering, Damanhour University, Egypt, is the sole case study, treated as an institutional educational facility as shown in **Figure 1**. The study boundary covers the complete building geometry modeled in DesignBuilder, while PV installation is limited to the façade identified through annual solar-radiation screening. Four repeated collector surfaces, each approximately 72 m long and 3.9 m high, provide a gross modeled façade allocation of 1,123.20 m². Architectural views document the building and façade organization, while the DesignBuilder model defines the simulation boundary. This allocation remains constant across all cases, enabling comparison of module performance and inclination without altering building geometry or available façade area.

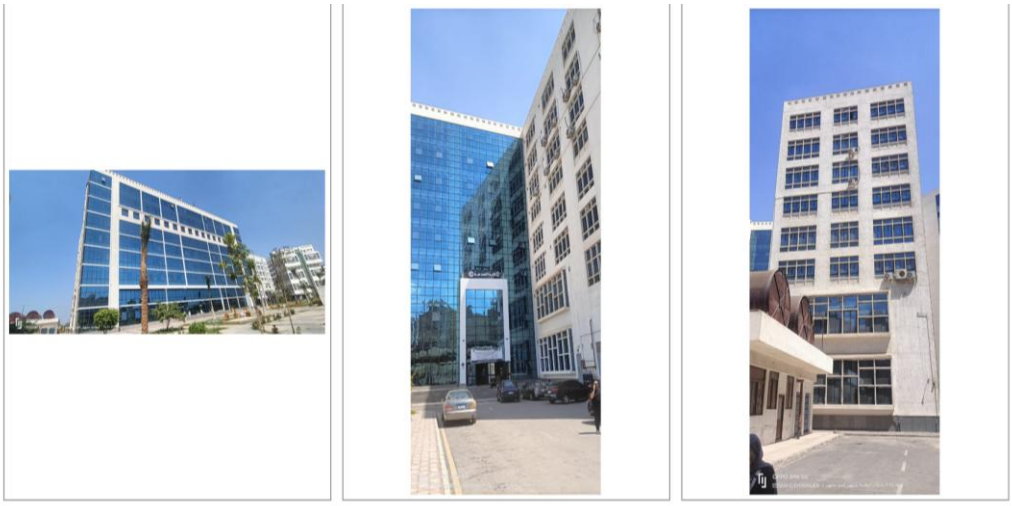

Figure 1. Photographic documentation of the Faculty of Engineering, Damanhour University, showing the existing main entrance and glazed façade, the repeated-window façade wing, and an additional courtyard/façade view.

The available DesignBuilder/EnergyPlus model represents a total and conditioned building area of 23,171.63 m². Four repeated floor-level PV collector surfaces, each approximately 72 m long and 3.9 m high, define the common gross

modeled façade allocation of 1,123.20 m². E01 is retained as the principal vertical façade identified by the annual solar-radiation screening, while the same four-collector allocation is maintained across the comparative PV scenarios to isolate module performance and inclination effects.

2.1. Building description and architectural representation

The Faculty of Engineering, Damanhour University, is documented through architectural/site drawings, photographs, and the DesignBuilder/EnergyPlus model as shown in **Figure 2**. Its modeled total and conditioned area is 23,171.63 m². The multi-zone educational building comprises a prominent blue glazed entrance block and adjacent opaque wings with repetitive rectangular windows, a paved forecourt, and projecting external air-conditioning units. These photographs document the existing envelope. For solar assessment, the envelope was divided into vertical surfaces E01–E20, with the roof as an additional reference. PV installation is restricted to façade E01. The common simulation allocation comprises four repeated floor-level collector surfaces, each approximately 72 m long and 3.9 m high, totaling 1,123.20 m². The architectural, photographic, and model views clarify the building geometry, existing façade condition, surface organization, and simulation boundary.

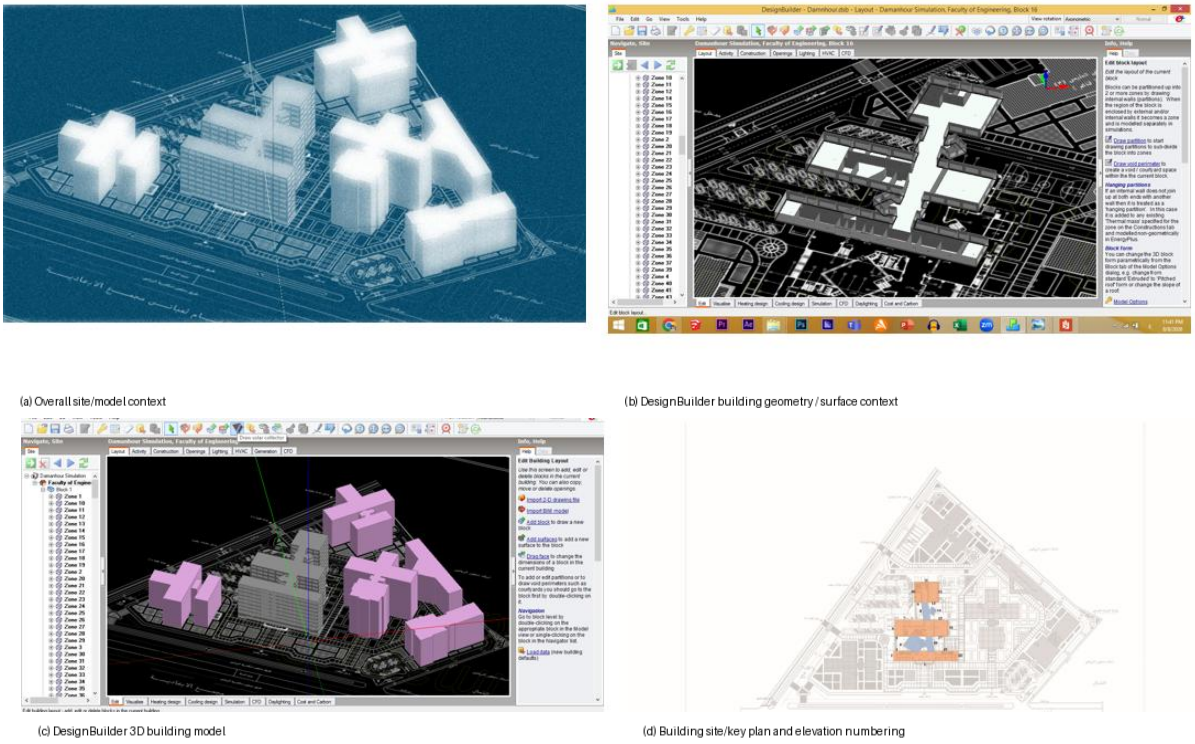

Figure 2. Architectural and DesignBuilder representation of the Faculty of Engineering, Damanhour University: (a) overall site/model context; (b) building geometry and surface context; (c) three-dimensional DesignBuilder model; and (d) site/key plan used for façade/elevation identification.

2.2. Climatic and simulation context

The annual building simulations were performed using the supplied EGY ETMY weather file identified by WMO station number "624200 Beheira". This file was used consistently throughout the 8,760-hour baseline and photovoltaic scenarios to maintain a common climatic boundary condition for comparative analysis. However, the reference weather station does not necessarily represent the exact meteorological conditions at the Faculty of Engineering, Damanhour University. Therefore, the simulated annual energy and PV outputs should be interpreted as estimates conditional on the selected weather file rather than as site-calibrated predictions. The use of a non-site-specific weather file is acknowledged as a source of uncertainty, and future work should evaluate the sensitivity of the results to a Damanhour-specific weather dataset.

2.3. Building-energy baseline

The baseline annual simulation reports 5,145,735.60 kWh/year of Total Site Energy and a Total Site EUI of 222.07 kWh/m²·year. Grid electricity demand is 1,149,629.45 kWh/year. District cooling is the dominant end-use at

3,893,520.27 kWh/year, followed by interior lighting at 1,001,709.56 kWh/year and interior equipment (reported by DesignBuilder as Building Electricity) at 147,919.89 kWh/year. District heating is comparatively smaller at 104,393.77 kWh/year. For the end-use-specific PV coverage calculation introduced below, the annual Building Electricity reference is taken from the complete twelve-month DesignBuilder monthly profile rather than the previously used July-only annualization. The monthly profile is shown in **Table 2**, and the corresponding DesignBuilder output is reproduced in **Figure 3** and **Table 3**.

Table 2. Monthly DesignBuilder Building Electricity consumption used to establish the annual end-use-specific reference demand.

Month	Building Electricity (MWh)	Building Electricity (kWh)
January	13.11	13,110
February	11.98	11,980
March	12.55	12,550
April	12.33	12,330
May	13.31	13,310
June	11.41	11,410
July	11.67	11,670
August	11.67	11,670
September	11.25	11,250
October	13.71	13,710
November	12.61	12,610
December	12.31	12,310
Annual total	147.91	147,919.89

The monthly values in **Table 2** are the Building Electricity values displayed by DesignBuilder for the twelve calendar months. Their rounded sum is 147.91 MWh/year, while the annual EnergyPlus/DesignBuilder utility report gives the corresponding interior-equipment total as 147,919.89 kWh/year. The July value of 11.67 MWh is consistent in magnitude with the previously reported July reference of 11,666.67 kWh/month; however, the revised calculation uses all twelve simulated months rather than multiplying July by twelve.

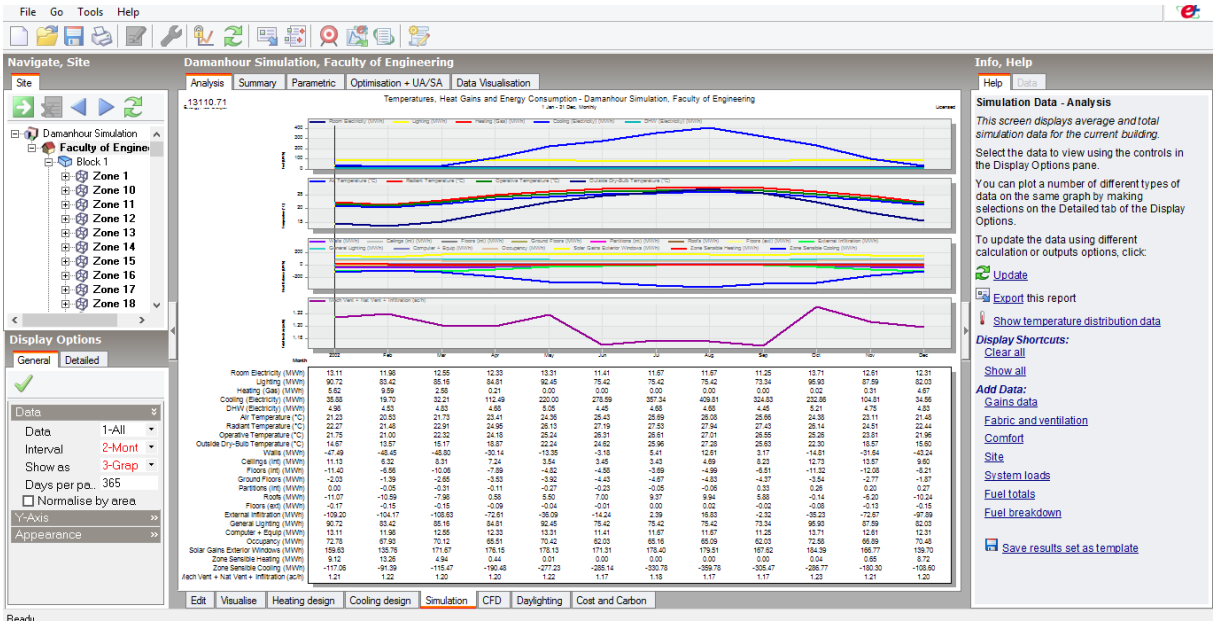

Figure 3. DesignBuilder monthly simulation output showing Building Electricity, lighting, cooling, heating, DHW, and related monthly energy indicators for the Damanhour Faculty of Engineering model.

Table 3. EUI Results

Baseline indicator	Value
Total Site Energy	5,145,735.60 kWh/year

Baseline indicator	Value
Total Site EUI	222.07 kWh/m²·year
Grid electricity	1,149,629.45 kWh/year
District cooling	3,893,520.27 kWh/year
Interior lighting	1,001,709.56 kWh/year
Interior equipment	147,919.89 kWh/year
District heating	104,393.77 kWh/year

3. MATERIALS AND METHODS

The revised methodology separates four evidence layers: (1) direct field electrical measurements, (2) weather-adjusted component-level electrical time series, (3) annual DesignBuilder/EnergyPlus building simulation, and (4) lifecycle economic screening. The hierarchy is intentional. The field test establishes observed electrical behavior; the weather-adjusted dataset examines temporal and inclination effects; the annual simulation determines whole-building consequences; and the economic model converts modeled grid reduction into investment indicators.

3.1. PV modules and field-test configuration

Two PV module options were investigated. JSM-195SP is a 195 W monocrystalline module with a nominal maximum-power voltage of 26.0 V, maximum-power current of 7.50 A, open-circuit voltage of 32.4 V, short-circuit current of approximately 8.02 A, and an approximate module area of 1.01 m². JS-190W-Special is treated using its reported 190 W rating and 1.25 × 1.25 m module area; the corresponding equivalent modeled efficiency is 12.16%. The annual DesignBuilder comparison uses 19.5% for JSM-195SP and 12.16% for JS-190W-Special.

Figure 4 and **Figure 5** show representative photographs of both investigated modules, documenting the physical modules used as the basis for comparative assessment. The building-energy model incorporates the photovoltaic module specifications to represent two alternative façade-integrated PV configurations: JSM-195SP and JS-190W-Special. The rated power and physical dimensions characterize the respective modules, while the conversion efficiency and active-cell fraction define the PV parameters adopted in the simulation. These parameters serve different purposes within the model and were therefore treated as separate inputs rather than interchangeable quantities. The annual electricity yield was calculated using DesignBuilder/EnergyPlus based on the selected module representation, façade configuration, and modeled PV parameters **Figure 6.** Accordingly, the comparison between the two module types reflects their performance under the modeling assumptions adopted in this study **Table 4**.

Table 4. PV Modules description

Parameter	JSM-195SP	JS-190W-Special
Nominal module rating	195 W	190 W
Modelled cell efficiency	19.5%	12.16%
Approx. module area	1.01 m²	1.5625 m²
PV representation in DesignBuilder	Simple PV	Simple PV
Active surface fraction	0.90	0.90
PV collector count	4	4
Electrical bus	DC	DC
Load centre / inverter	DC with inverter	DC with inverter

Figure 4. Jet Solar JSM-195SP module used for the localized electrical field test at the Damanhour study site.

Figure 5. JA Solar JS-190W-Special module used as the second PV option in the comparative field and simulation assessment.

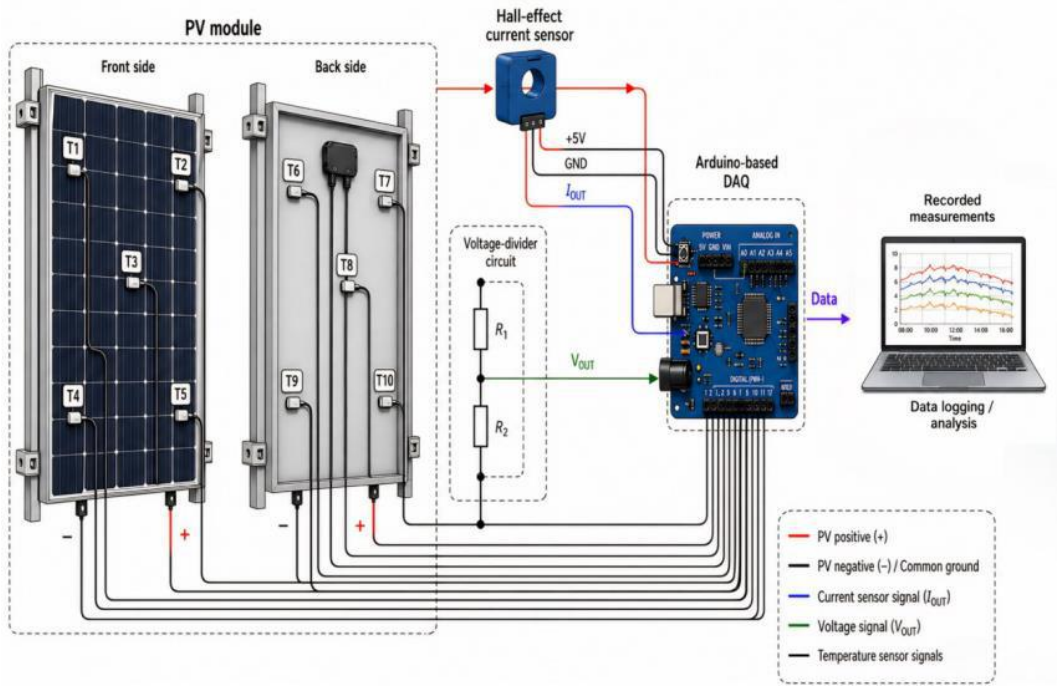

Figure 6. Experimental PV monitoring and data-acquisition arrangement used for current/power characterization.

The field campaign reported in the supplied Damanhour assessment was conducted on 2 July 2026. The conventional PV test was sampled at 30-minute intervals from 07:00 to 17:30. A separate BIPV test contained two measured points, for which the supplied report uses the arithmetic mean while retaining the limited two-point nature of the measurement. The measurements are therefore treated as direct observations of electrical behavior rather than as an annual-yield dataset as shown in **Figures 7 and 8.**

3.2. Field-test data treatment

Instantaneous power was calculated as ($P(t)=V(t)I(t)$). Field analysis examined temporal current and power patterns, including morning increases, midday peaks, afternoon declines, and local obstruction effects **Table 5**. The measurements were not used to calibrate the annual building-energy model because complete annual utility data were unavailable. Therefore, ASHRAE Guideline 14 metrics (NMBE and CV(RMSE)) are not reported.

Table 5. Field Test results

Field test	Mean current (A)	Peak current (A)	Mean power (W)	Peak power (W)
Conventional PV test — 2 July 2026	2.72	3.57	41.42	54.33
BIPV test — mean of two measured points	8.05	8.50	89.79	94.50

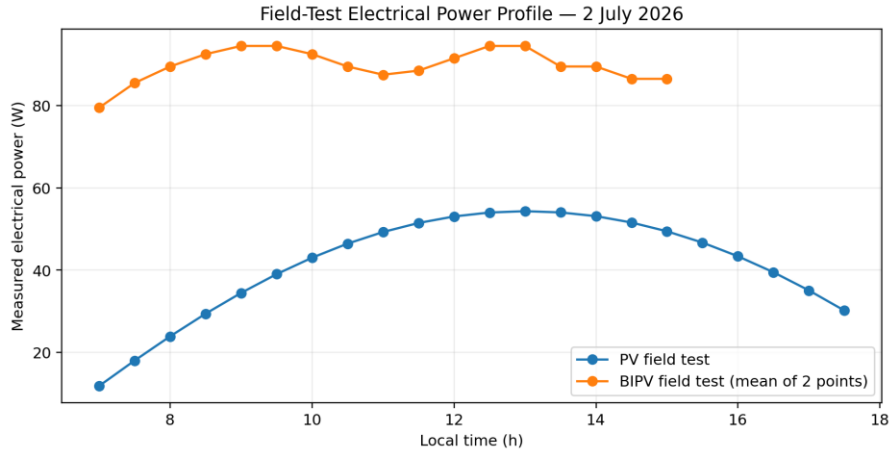

Figure 7. Measured electrical power profile during the 2 July 2026 field test; the separate BIPV test remains substantially higher over the recorded period.

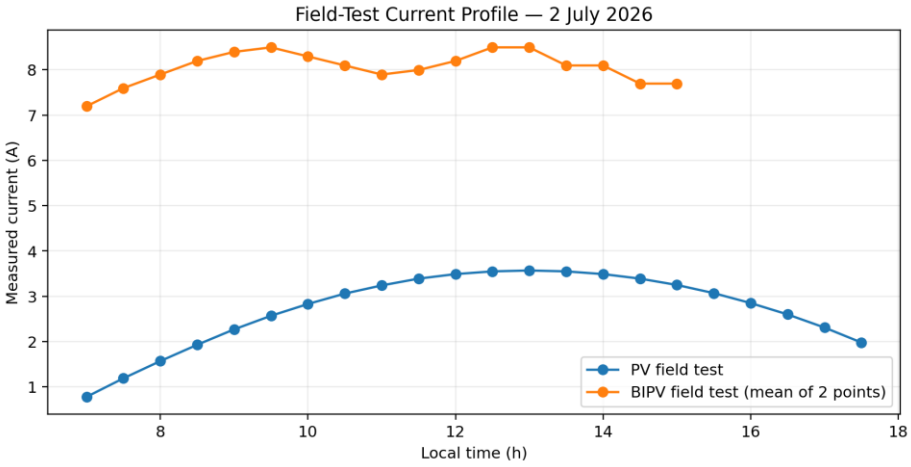

Figure 8. Measured current profile during the 2 July 2026 field test.

3.3. Weather-adjusted July–August electrical time series

The supplied spreadsheet contains 2,064 half-hour records for each of four configurations from 00:00 on 1 July through 23:30 on 12 August 2026 **Figure 9**. The cases are JSM-195SP at 90° and 30°, and JS-190W-Special at 90° and 30°. The dataset combines the supplied EPW weather variables with module-specific response constants established from the previous field-response treatment. The spreadsheet explicitly labels these values as synthetic/weather-adjusted estimates rather than measured readings or direct DesignBuilder hourly output. This distinction is retained in the manuscript.

Table 6. Module/tilting results

Module/tilt	Power-response constant (W per W/m² POA)	Equivalent voltage (V)	Rated power
JSM-195SP 90°	0.163732	15.209258	195 W
JSM-195SP 30°	0.163732	15.209258	195 W
JS-190W-Special 90°	0.344144	11.118056	190 W
JS-190W-Special 30°	0.344144	11.118056	190 W

The weather-adjusted series is used primarily to quantify the effect of inclination on plane-of-array irradiance and electrical-energy accumulation. It is not used to override the annual DesignBuilder ranking because the two analyses

use different electrical representations: the time series uses the supplied module-response constants, whereas the annual building model uses the controlled Simple PV efficiencies. This distinction is essential because the time-series dataset produces higher short-period electrical energy for JS-190W-Special, while the annual building simulation ranks JSM-195SP higher **Table 6**.

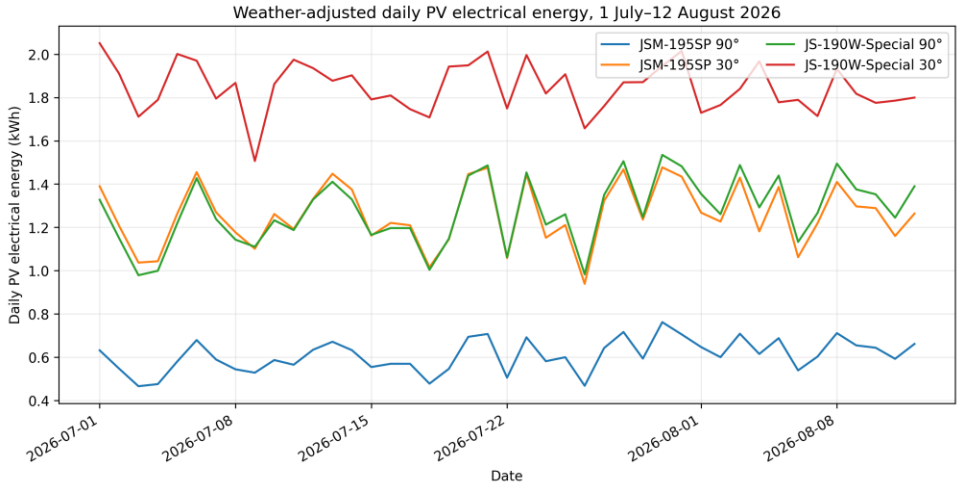

Figure 9. Weather-adjusted daily PV electrical-energy profiles for the four configurations from 1 July to 12 August 2026.

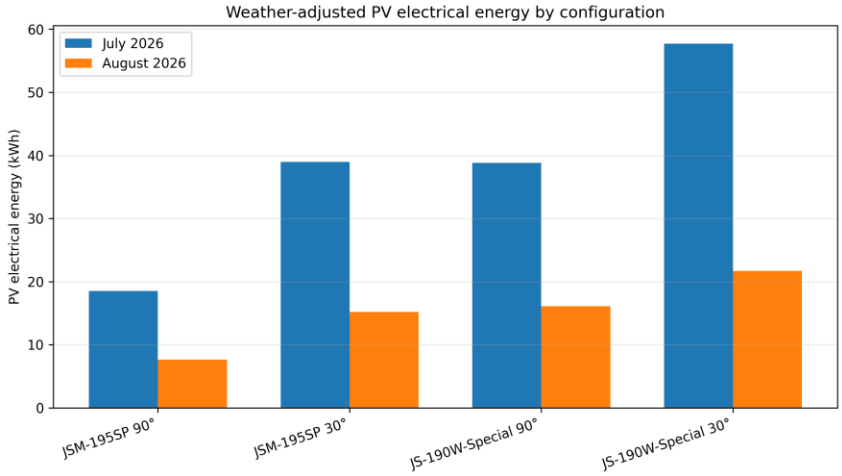

Figure 10. Weather-adjusted monthly PV electrical energy for July and August 2026.

3.4. Solar-radiation screening and façade selection

Building elevations were numbered E01–E20, with the roof as an additional reference surface. Monthly incident solar radiation was extracted from DesignBuilder for January–December. Monthly comparisons are presented in **Figure 10,** while annual cumulative rankings appear in the annual-ranking table and **Figure 11.** This screening identified the most suitable vertical façade based on the actual building geometry rather than generalized cardinal-orientation assumptions.

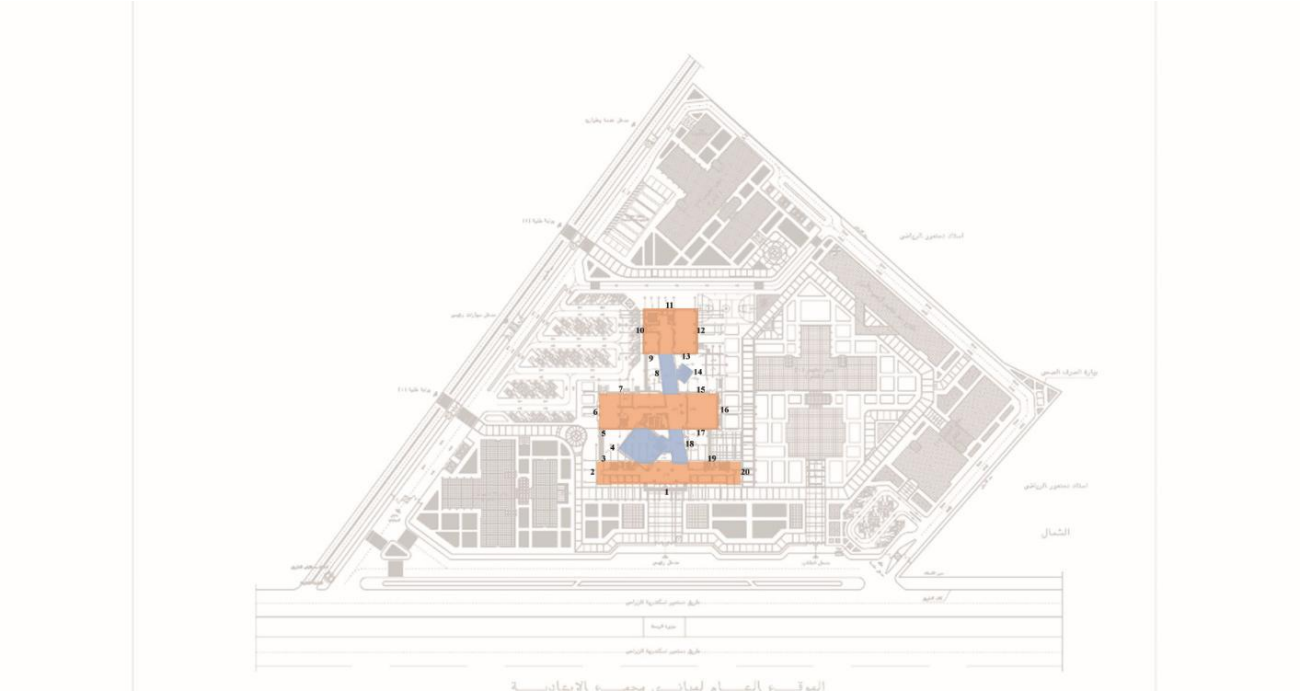

Figure 11. Building site/key plan showing the identified and numbered elevations used in the annual solar-radiation screening.

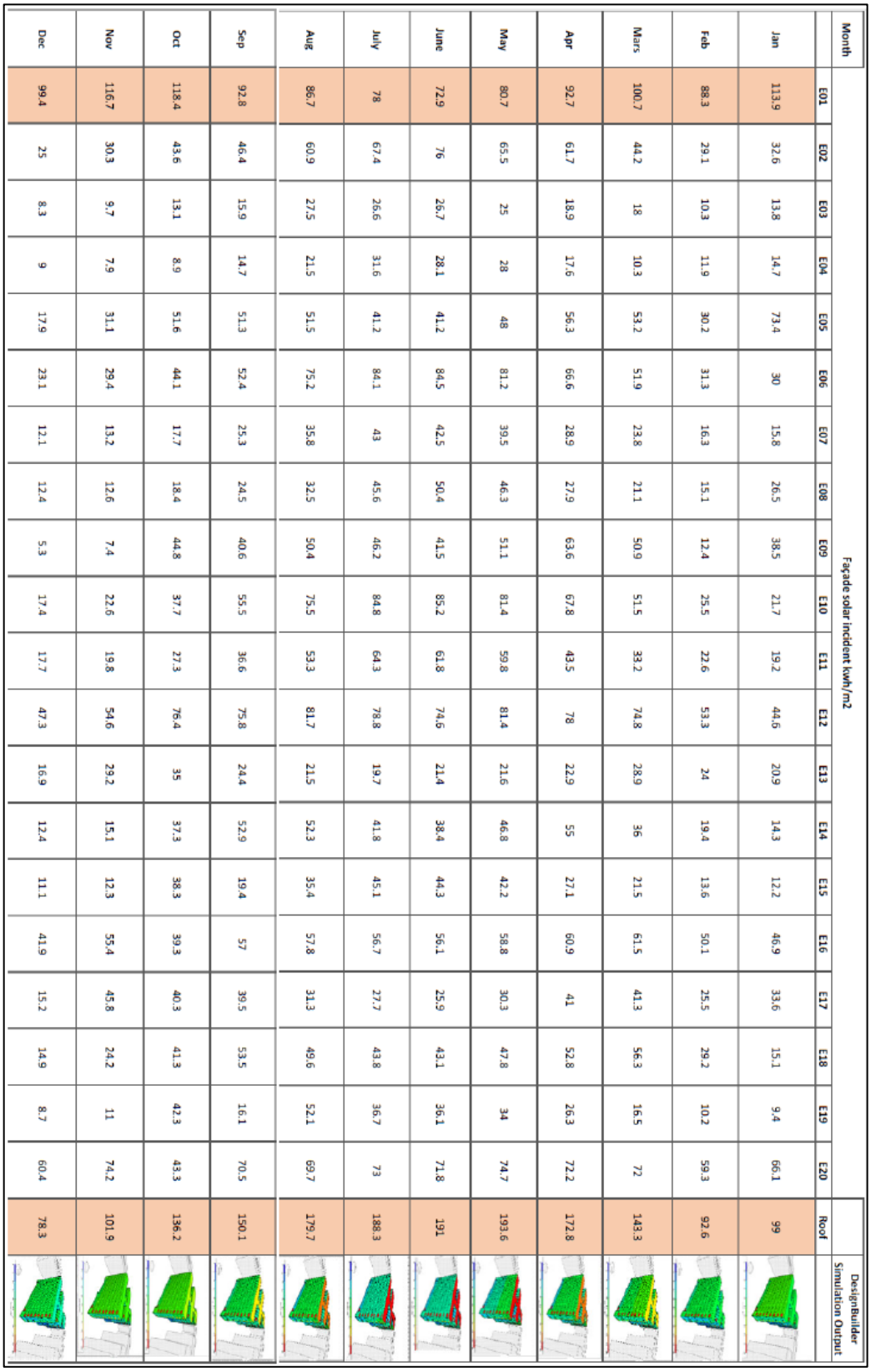

Month	Façade solar incident kwh/m2																			DesignBuilder Simulation Output
	E01	E02	E03	E04	E05	E06	E07	E08	E09	E10	E11	E12	E13	E14	E15	E16	E17	E18	E19	E20	Roof	
Jan	113.9	32.6	13.8	14.7	73.4	30	15.8	26.5	38.5	21.7	19.2	44.6	20.9	14.3	12.2	46.9	33.6	15.1	9.4	66.1	99	
Feb	88.3	29.1	10.3	11.9	30.2	31.3	16.3	15.1	12.4	25.5	22.6	53.3	24	19.4	13.6	50.1	25.5	29.2	10.2	59.3	92.6	
Mars	100.7	44.2	18	10.3	53.2	51.9	23.8	21.1	50.9	51.5	33.2	74.8	28.9	36	21.5	61.5	41.3	56.3	16.5	72	143.3	
Apr	92.7	61.7	18.9	17.6	56.3	66.6	28.9	27.9	63.6	67.8	43.5	78	22.9	55	27.1	60.9	41	52.8	26.3	72.2	172.8	
May	80.7	65.5	25	28	48	81.2	39.5	46.3	51.1	81.4	59.8	81.4	21.6	46.8	42.2	58.8	30.3	47.8	34	74.7	193.6	
June	72.9	76	26.7	28.1	41.2	84.5	42.5	50.4	41.5	85.2	61.8	74.6	21.4	38.4	44.3	56.1	25.9	43.1	36.1	71.8	191	
July	78	67.4	26.6	31.6	41.2	84.1	43	45.6	46.2	84.8	64.3	78.8	19.7	41.8	45.1	56.7	27.7	43.8	36.7	73	188.3	
Aug	86.7	60.9	27.5	21.5	51.5	75.2	35.8	32.5	50.4	75.5	53.3	81.7	21.5	52.3	35.4	57.8	31.3	49.6	52.1	69.7	179.7	
Sep	92.8	46.4	15.9	14.7	51.3	52.4	25.3	24.5	40.6	55.5	36.6	75.8	24.4	52.9	19.4	57	39.5	53.5	16.1	70.5	150.1	
Oct	118.4	43.6	13.1	8.9	51.6	44.1	17.7	18.4	44.8	37.7	27.3	76.4	35	37.3	38.3	39.3	40.3	41.3	42.3	43.3	136.2	
Nov	116.7	30.3	9.7	7.9	31.1	29.4	13.2	12.6	7.4	22.6	19.8	54.6	29.2	15.1	12.3	55.4	45.8	24.2	11	74.2	101.9	
Dec	99.4	25	8.3	6	17.9	23.1	12.1	12.4	5.3	17.4	17.7	47.3	16.9	12.4	11.1	41.9	15.2	14.9	8.7	60.4	78.3	

Figure 12. DesignBuilder monthly incident solar radiation matrix for elevations E01–E20 and the roof.

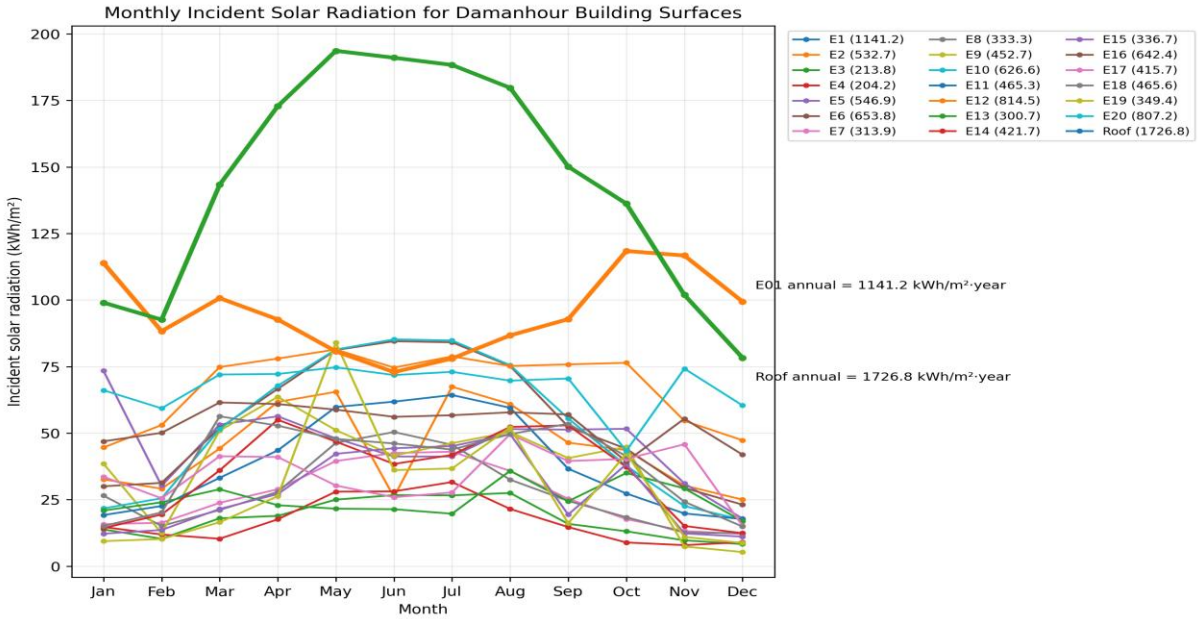

Figure 13. Complete January–December incident solar radiation trends for Elevations E01–E20 and the roof.

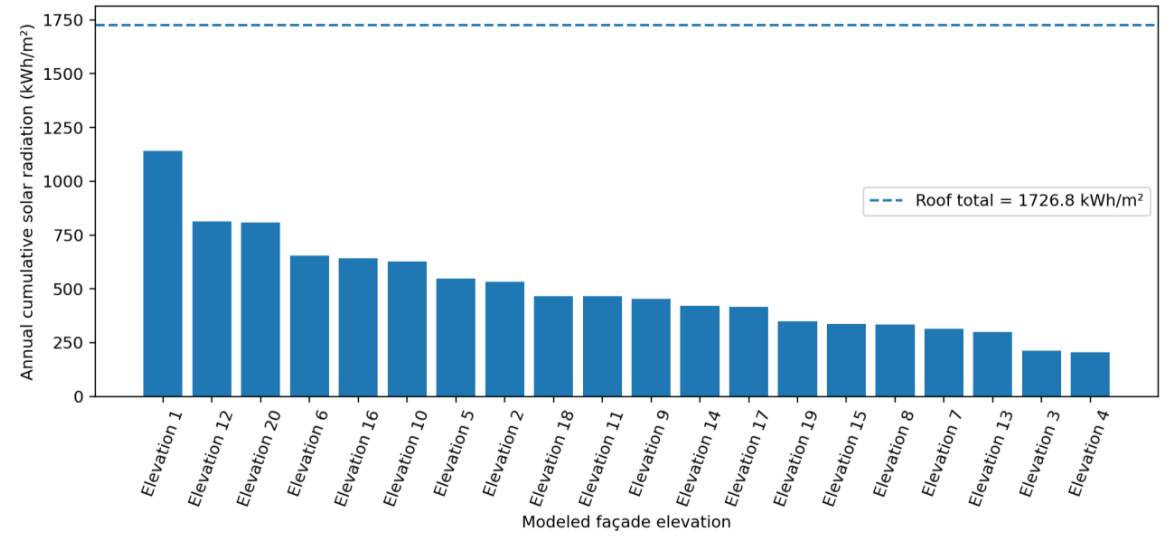

Figure 14. Annual cumulative incident solar-radiation ranking of the investigated Damanhour building surfaces.

Table 7. Complete annual cumulative incident solar-radiation ranking for the investigated Damanhour building surfaces.

Rank	Surface	Annual incident solar radiation (kWh/m²·year)	Interpretation
1	Roof	1726.8	Highest overall solar-receiving surface
2	E1	1141.2	Highest-performing vertical façade; selected for PV study
3	E12	814.5	Second-tier vertical candidate
4	E20	807.2	Second-tier vertical candidate
5	E6	653.8	Lower than E01 but among stronger vertical candidates
6	E16	642.4	Lower-performing vertical surface in annual screening
7	E10	626.6	Lower-performing vertical surface in annual screening
8	E5	546.9	Lower-performing vertical surface in annual screening
9	E2	532.7	Lower-performing vertical surface in annual screening
10	E18	465.6	Lower-performing vertical surface in annual screening
11	E11	465.3	Lower-performing vertical surface in annual screening
12	E9	452.7	Lower-performing vertical surface in annual screening
13	E14	421.7	Lower-performing vertical surface in annual screening
14	E17	415.7	Lower-performing vertical surface in annual screening
15	E19	349.4	Lower-performing vertical surface in annual screening
16	E15	336.7	Lower-performing vertical surface in annual screening
17	E8	333.3	Lower-performing vertical surface in annual screening
18	E7	313.9	Lower-performing vertical surface in annual screening
19	E13	300.7	Lower-performing vertical surface in annual screening
20	E3	213.8	Lower-performing vertical surface in annual screening
21	E4	204.2	Lower-performing vertical surface in annual screening

Elevation 1 (E01) is the strongest vertical façade, with 1,141.2 kWh/m²·year, while the roof remains the highest-radiation surface overall at 1,726.8 kWh/m²·year. E01 exceeds the roof in January, November, and December, whereas the roof dominates from February through October **Figures 12 to 14.** The complete annual ranking confirms that E01 is the leading vertical candidate, followed by E12 (814.5 kWh/m²·year) and E20 (807.2 kWh/m²·year). Because the study specifically evaluates façade-applied PV, E01 is selected as the principal façade for the controlled PV simulations rather than selecting the roof solely based on its higher annual radiation **Table 7**.

3.5. DesignBuilder modelling and simulation workflow evidence

DesignBuilder photo captions document the 3D building/site model and zone hierarchy, building inputs, PV/electrical-system parameters, and annual, monthly, and surface-level output settings. Solar screening used surface-output storage and solar-incident reporting to assess the roof and numbered façades throughout the year **Figure 15.** All four PV configurations retained the same model boundary and simulation framework, with module performance and collector inclination as controlled variables. The captions document the modelling workflow, not additional simulation runs.

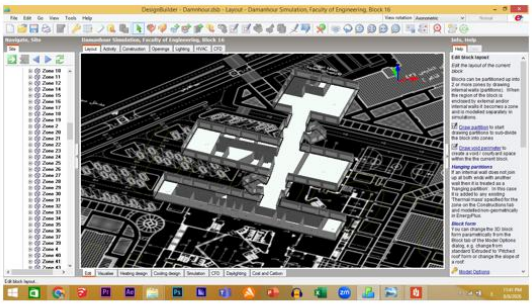

(a) Calculation/output options and model context

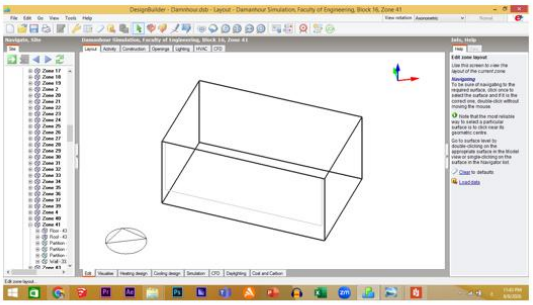

(b) Initial geometric block representation

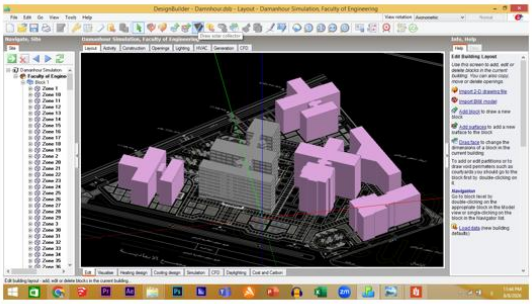

(c) Complete building model and zone hierarchy

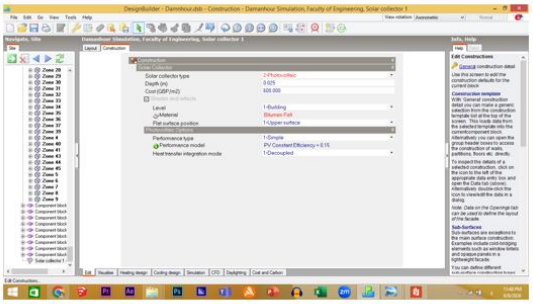

(d) Building input/template definition

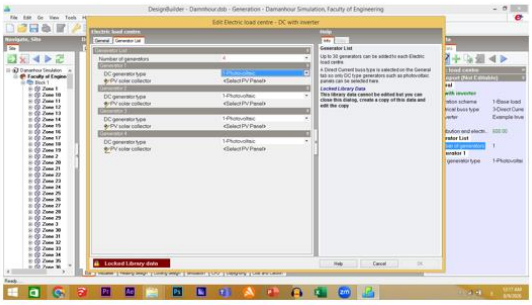

(e) PV/electrical-system definition

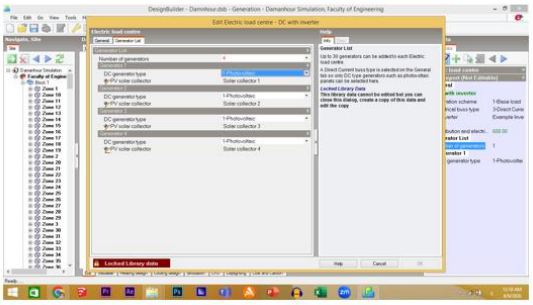

(f) PV performance parameters

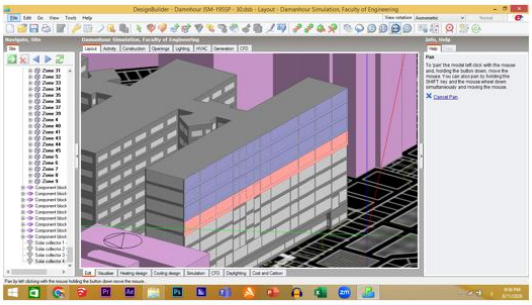

(g) EnergyPlus calculation/output selection

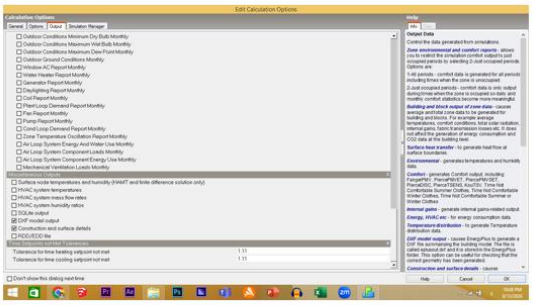

(h) Monthly output/reporting selection

Figure 15. DesignBuilder workflow evidence used to document the building representation, model inputs, PV/electrical-system definition, and annual calculation/output configuration.

Simulation Workflow

1) Building geometry and thermal-zone hierarchy → Establish the building geometry, physical massing, surface definitions, and thermal-zone structure.

2) Building inputs and templates → Retain and verify the specified constructions, occupancy activities, schedules, internal loads, and HVAC definitions.

3) Surface configuration and solar-radiation outputs → Configure the façade and roof surfaces for solar screening, and enable the required surface outputs, including incident solar radiation.

4) Photovoltaic (PV) system definition → Define the four façade PV collectors, the Simple PV performance model, active-cell area fraction, DC electrical bus, and inverter/load-center arrangement.

5) PV module performance cases → Implement the JSM-195SP and JS-190W-Special module performance inputs while maintaining consistent model boundaries and assumptions across the comparative cases.

6) Inclination cases → Evaluate the original vertical configuration and the 30° inclined configuration while keeping other simulation parameters consistent.

7) Annual simulation and reporting → Perform the controlled annual EnergyPlus simulations and extract the relevant building energy, grid electricity, thermal-performance, and PV-generation outputs.

3.6. Controlled Design Builder/Energy-Plus building simulation

The building energy model was developed in DesignBuilder using EnergyPlus and the existing Faculty of Engineering, Damanhour University geometry, including floor area, thermal zones, envelope, occupancy schedules, lighting, equipment, domestic hot water, and HVAC systems. Annual 8,760-hour simulations used the EGY ETMY weather file (WMO 624200) consistently. The selected façade was modeled using four repeated PV collector surfaces, each approximately 72 m × 3.9 m, totaling 1,123.20 m². Collectors used the Simple PV representation with a 0.90 active-cell fraction. Two module cases were assessed: JSM-195SP (19.5% efficiency) and JS-190W-Special (12.16%). The electrical system comprised a DC bus and DC-with-inverter load center, with continuous PV availability. Across all four scenarios, building geometry, façade allocation, weather, simulation period, collector count, active fraction, and electrical configuration remained constant; module performance and inclination were the controlled variables. The original vertical façade (90°) was compared with a 30° inclination. This consistent framework enabled assessment of annual PV generation, building energy demand, and grid-electricity consumption **Tables 8 and 9**. The 30° inclination was examined as an alternative to the 90° vertical façade configuration to evaluate how the modeled orientation affects annual PV electricity generation and the associated building-energy outcomes. Including both configurations enables a comparative assessment under the same weather file and building-energy modeling framework. The 30° case is therefore treated as an alternative modeled configuration, while the 90° case represents the vertical façade arrangement. The comparison focuses on simulated energy performance; the feasibility of a specific installation also depends on the structural and architectural conditions of the façade.

Table 8. Tilting Scenarios

Scenario	PV module	Tilt/Configuration	Role
S0	None	Baseline	Reference
S1	JSM-195SP	90°	Vertical façade condition
S2	JS-190W-Special	90°	Vertical façade condition
S3	JSM-195SP	30°	Tilted configuration
S4	JS-190W-Special	30°	Tilted configuration

Table 9. Simulation Configurations and setup

Common input	Controlled value
Building	Faculty of Engineering, Damanhour University
Total/conditioned area	23,171.63 m²
Simulation period	8,760 h
Weather file	Beheira EGY ETMY, WMO 624200
PV façade allocation	4 repeated floor-level collector surfaces

Common input	Controlled value
Repeated façade length	72 m
Repeated floor height	3.9 m
Gross modeled PV allocation	1,123.20 m²
Active surface fraction	0.90
PV collector count	4
Electrical bus	DC
Load centre / inverter	DC with inverter
PV availability	On 24/7

The annual PV output is therefore generated inside the building simulation rather than obtained from a simple annual specific-yield multiplication. This directly addresses the methodological limitation identified during review. The field-test measurements remain an empirical reference for electrical behavior, while the annual EnergyPlus outputs provide the evidence for building-scale PV generation, grid reduction, and thermal interaction.

3.7. Economic methodology

The economic analysis uses project-specific commercial inputs for the Damanhour case: an institutional electricity tariff of 1.95 EGP/kWh, a module price of 6,000 EGP/panel for JSM-195SP, and 12,000 EGP/panel for JS-190W-Special. The physical/layout-equivalent panel counts used for the common modeled façade allocation are approximately 462 JSM-195SP panels and 1,112 JS-190W-Special panels. Accordingly, the module-only CAPEX screening values are 2.772 million EGP and 13.344 million EGP, respectively. These values cover the module purchase cost only and do not represent a complete EPC/BIPV installed cost; inverter, mounting/substructure, wiring, protection, installation, maintenance, replacement, and other balance-of-system costs are excluded because no verified project-specific quotations were supplied. The economic comparison therefore reports a transparent module-cost simple payback rather than an investment-grade full-system payback.

Annual avoided electricity-cost value = annual net grid reduction × electricity tariff (1)

$$Annual\ O\&M = 0.012 \times CAPEX \quad (2)$$

$$E_t = E_1 \times (1 - d)^{(t-1)} \quad (3)$$

$$CF_t = (Eoffset,_t \times Rgrid) - CO\&M \quad (4)$$

$$NPV = -CAPEX + \Sigma[CF_t / (1+r)^t] \quad (5)$$

$$IRR\ solves:\ 0 = -CAPEX + \Sigma[CF_t / (1+IRR)^t] \quad (6)$$

$$LCOE = [CAPEX + \Sigma(CO\&M/(1+r)^t)] / \Sigma[Eoffset,_t/(1+r)^t] \quad (7)$$

The revised simple-payback calculation uses the modeled annual net grid reduction rather than gross PV generation, because the former represents the simulated reduction in purchased grid electricity. Simple payback is calculated as module-only CAPEX divided by annual avoided electricity-cost value. The resulting figures are intentionally described as module-cost screening paybacks because balance-of-system and installation costs are not included.

4. RESULTS AND DISCUSSION

4.1. Measured field electrical performance

The 2 July 2026 field test provides direct experimental supporting evidence for the electrical behavior of the investigated PV systems. The conventional PV test reached 54.33 W peak power and 3.57 A peak current at approximately 13:00, while its mean power and current were 41.42 W and 2.72 A. The separate two-point BIPV test reached 94.50 W peak power and 8.50 A peak current, with mean values of 89.79 W and 8.05 A. These measurements demonstrate the daylight-dependent response of current and power and provide an empirical reference for interpreting the modeled electrical behavior.

The field test therefore supports H1 as experimental evidence. It confirms the expected temporal variation of current and power and strengthens the physical interpretation of the subsequent simulation results. Because the campaign was limited in duration and did not provide a complete annual building-electricity metering dataset, it is not used as a direct annual-yield calibration dataset and does not support annual NMBE/CV(RMSE) validation. The validation scope is limited to the measured electrical response of the tested PV systems under the observed field conditions. A statistical comparison between measured and simulated annual building energy use could not be conducted because a corresponding annual utility-meter dataset was not available. Accordingly, NMBE and CV(RMSE) are not reported, since calculating these indicators requires paired measured and simulated values for a comparable variable, time interval, and system boundary. The field measurements are therefore treated as experimental supporting evidence for component-level electrical behavior, while the annual building-energy results remain simulation-based estimates. This distinction avoids presenting short-duration electrical measurements as validation of annual whole-building energy consumption.

4.2. Weather-adjusted electrical response and inclination effect

The weather-adjusted July–August series provides a second level of evidence. For JSM-195SP, July electrical energy increases from 18.51 kWh at 90° to 38.96 kWh at 30°, an increase of 110.5%; the corresponding August increase is 98.3%. For JS-190W-Special, the increase is 48.7% in July and 34.8% in August. The same directional effect is visible in the daily profiles, confirming that the 30° inclination improves plane-of-array solar collection during the investigated summer period. The electrical data presented for the July - August period represent a weather-adjusted estimate based on the supplied EPW weather data and the adopted PV performance assumptions, rather than a continuous record of direct field measurements. Direct experimental measurements were collected during the field test conducted on 2 July 2026. The weather-adjusted series extends the analysis beyond the measurement period and provides a consistent basis for examining the estimated electrical response under the selected weather conditions. Accordingly, the field measurements and the weather-adjusted estimates serve complementary roles in the assessment of the two PV configurations.

The weather-adjusted dataset and annual DesignBuilder simulation serve different purposes. Derived from EPW weather and module-response constants, the time series represents temporal electrical behavior, whereas the controlled Simple PV model evaluates whole-building impacts. These datasets should remain separate to avoid treating the short-period electrical model as direct annual monitoring. The experimental measurements, weather-adjusted electrical estimates, and annual building-energy simulations represent different stages of the assessment. The field measurements provide direct evidence of PV electrical behavior under the observed test conditions, whereas the weather-adjusted series estimates the electrical response over the selected period using the adopted weather data and PV assumptions. The DesignBuilder/EnergyPlus simulations extend the analysis to annual PV generation and building-energy performance under a consistent set of modeled conditions. The three datasets are therefore interpreted according to their respective temporal coverage and assessment boundaries. Because a corresponding annual measured building-energy dataset was not available, the comparison does not constitute a statistical validation of annual whole-building energy predictions.

4.3. Solar-resource-based façade selection

The solar-radiation screening identifies E01 as the leading vertical façade. Its annual incident radiation of 1,141.2 kWh/m²·year is approximately 66.1% of the roof value of 1,726.8 kWh/m²·year. The result also varies seasonally: E01 exceeds the roof in January, November, and December, illustrating why monthly rather than single-month or orientation-only screening is preferable for façade selection.

The solar screening supports H4 by demonstrating that façade selection should be based on the simulated solar resource at the actual building surfaces. E01 records 1,141.2 kWh/m²·year, making it the highest-performing vertical façade, whereas the roof reaches 1,726.8 kWh/m²·year and is the highest surface overall. E01 exceeds the roof in January, November, and December, while the roof dominates from February through October. Because the research question is specifically concerned with façade-applied PV, E01 is selected as the principal façade to maintain a like-for-like vertical comparison. This selection avoids substituting the roof simply because it has a higher global radiation value.

4.4. Five-scenario annual DesignBuilder/EnergyPlus performance

The five-scenario annual Total Site Energy and Net Site Energy comparison from the controlled DesignBuilder/EnergyPlus simulations is shown in **Figure 16.**

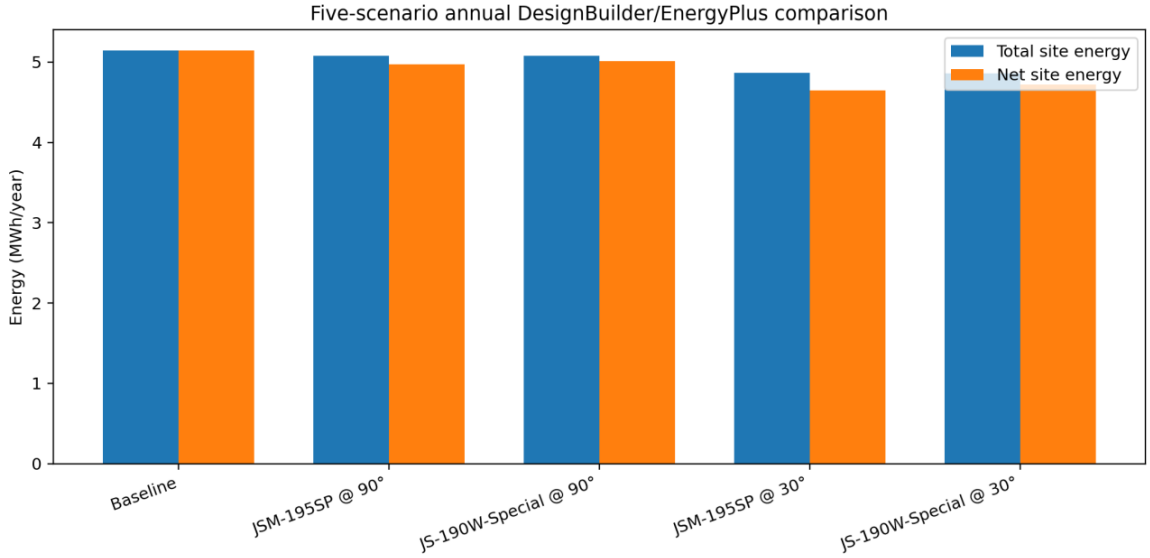

Figure 16. Five-scenario annual Total Site Energy and Net Site Energy comparison from the controlled DesignBuilder/EnergyPlus simulations.

Table 10. Simulation Results

Scenario	PV generation (kWh/yr)	Total Site Energy (kWh/yr)	Net Site Energy (kWh/yr)	Net EUI (kWh/m²·yr)	Net grid reduction (kWh/yr)	Grid reduction
Baseline @ —	0.00	5,145,735.60	5,145,735.60	222.07	0.00	0.00%
JSM-195SP @ 90°	109,132.83	5,077,733.70	4,974,057.51	214.66	103,676.19	9.02%
JS-190W-Special @ 90°	68,054.12	5,077,733.70	5,013,082.29	216.35	64,651.41	5.62%
JSM-195SP @ 30°	229,119.60	4,868,157.30	4,650,493.68	200.70	217,663.62	18.93%
JS-190W-Special @ 30°	147,994.92	4,859,968.56	4,719,373.39	203.67	140,595.18	12.23%

The annual energy results distinguish between gross PV electricity generation and the reduction in grid-electricity demand relative to the baseline case. Gross PV generation represents the electricity output attributed to the modeled photovoltaic system, whereas net grid-electricity reduction represents the difference between the baseline and the corresponding PV scenario. These indicators are reported separately because they describe different energy quantities and assessment boundaries. The comparison between the baseline and PV cases also reflects the building-energy outputs associated with each modeled configuration. Accordingly, PV generation is not treated as automatically equivalent to the reduction in grid-electricity demand **Figures 17 and 18**. The baseline consumes 5,145,735.60 kWh/year. The vertical JSM-195SP and JS-190W-Special cases produce 109.13 and 68.05 MWh/year of PV electricity, reducing net grid electricity by 103.68 and 64.65 MWh/year, respectively. Changing the collector inclination to 30° produces a major improvement: JSM-195SP reaches 229.12 MWh/year and 18.93% grid reduction, while JS-190W-Special reaches 147.99 MWh/year and 12.23% grid reduction.

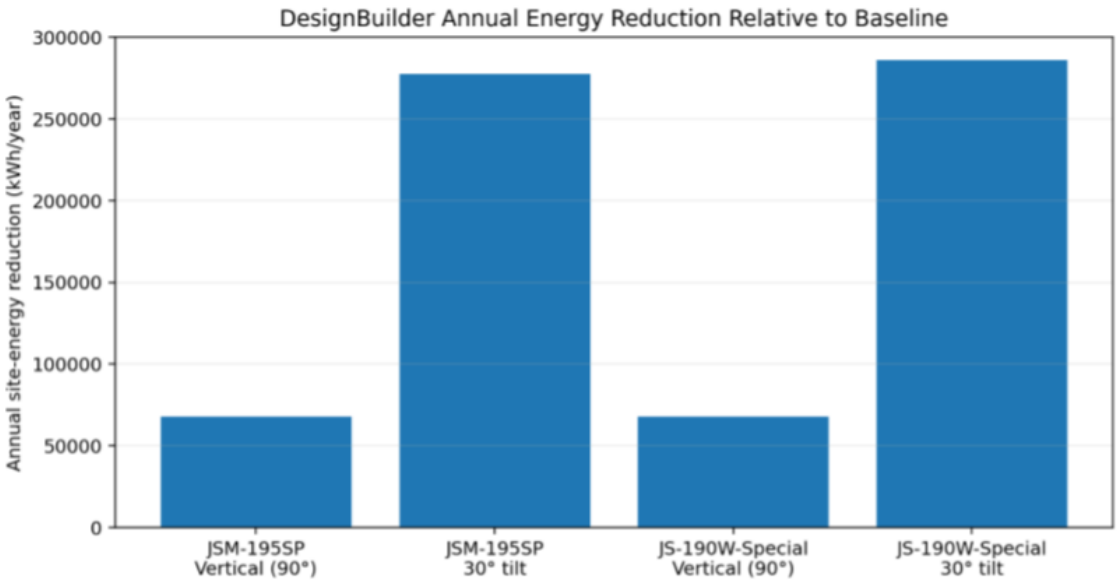

Figure 17. Annual total-site energy reduction relative to the Damanhour baseline for the four PV configurations.

The 30° JSM-195SP case is the strongest overall building-energy configuration. Its Net Site Energy is 4,650,493.68 kWh/year, and its Net EUI is 200.70 kWh/m²·year. The JS-190W-Special at 30° produces a slightly lower gross Total Site Energy of 4,859,968.56 kWh/year compared with 4,868,157.30 kWh/year for JSM-195SP at 30°. However, this 8,188.74 kWh/year gross difference is only about 0.17% of the baseline and does not outweigh the substantially higher PV generation, lower Net Site Energy, lower Net EUI, and higher grid reduction of JSM-195SP. The preferred scenario is therefore selected using a multi-metric decision basis rather than gross Total Site Energy alone.

4.4.1. Monthly electricity-demand reference and PV coverage

The monthly DesignBuilder profile established an annual Building Electricity reference of 147,919.89 kWh/year for PV panel sizing. This model-derived end-use reference is distinct from whole-building grid electricity. The theoretical panel count equals this annual demand divided by simulated annual PV production per panel; the practical count is rounded up to the next whole panel. These sizing calculations do not represent additional DesignBuilder simulations.

The annual Building Electricity value of 147,919.89 kWh/year is used as an end-use-specific reference for the practical PV sizing exercise. It is distinct from the modeled annual grid-electricity demand of 1,149,629.45 kWh/year and from the building's total annual site energy consumption. Consequently, the practical panel count calculated to offset the Building Electricity reference represents an end-use-based sizing scenario, not a configuration that offsets the building's entire annual energy demand. Whole-building performance is evaluated separately using the annual energy balance and net grid-electricity results reported in **Tables 10 and 11**.

Table 11. Panel productivity derived from the controlled annual simulations.

Scenario	Modeled panels	Annual PV generation (kWh/yr)	PV production per panel (kWh/panel·yr)	Equivalent average power per panel (W)
JSM-195SP @ 90°	462	109,132.83	236.22	26.97
JS-190W-Special @ 90°	1,112	68,054.12	61.20	6.99
JSM-195SP @ 30°	462	229,119.60	495.93	56.61
JS-190W-Special @ 30°	1,112	147,994.92	133.09	15.19

The façade PV assessment distinguishes between the gross geometric area allocated to the modeled collector surfaces, the active area represented in the PV model, and the physical area occupied by the selected modules. These quantities describe different aspects of the installation: the gross façade area defines the available geometric envelope, the active-area fraction represents the portion assigned to PV collection, and the module dimensions determine the physical area required for a given panel count. The practical sizing results are therefore interpreted in relation to both the annual

electricity-generation target and the corresponding module-area requirement, rather than treating the gross façade area and the total physical module area as equivalent quantities.

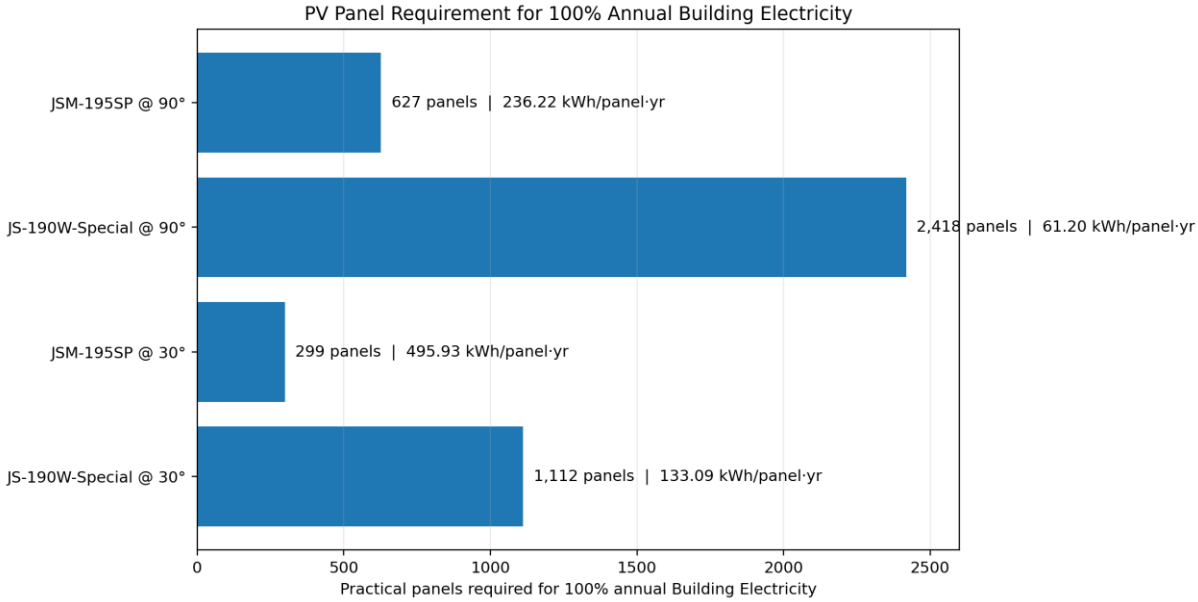

Figure 18. Practical PV panel count required to reach 100% of the adopted annual Building Electricity reference.

The resulting practical 100% requirements are 627 JSM-195SP panels at 90°, 2,418 JS-190W-Special panels at 90°, 299 JSM-195SP panels at 30°, and 1,112 JS-190W-Special panels at 30°. The 30° JSM-195SP case therefore reaches the adopted annual Building Electricity target with the smallest practical panel count. The 90° configurations require larger panel allocations, and where their calculated requirement exceeds the currently studied façade allocation, the additional modules would be distributed across adjacent suitable façades rather than concentrated on the principal studied façade. This sizing result should not be interpreted as a whole-building NZEB claim; whole-building grid reduction remains the separate building-scale metric. The corresponding equivalent PV areas are 1,524.34 m², 2,442.35 m², 726.92 m², and 1,123.20 m², respectively, relative to the 1,123.20 m² studied façade allocation.

4.5. Thermal and environmental performance

The annual simulations indicate a measurable thermal interaction between the façade PV intervention and building cooling demand. JSM-195SP at 30° reduces annual district cooling by 288.36 MWh/year (7.41%), while JS-190W-Special at 30° reduces it by 296.92 MWh/year (7.63%). These are model-specific results and should not be generalized as a universal PV thermal benefit because the thermal effect depends on façade construction, PV attachment, air cavities, shading geometry, and boundary conditions **Table 12**. The simulated district-cooling results show a difference between the baseline building and the PV scenarios, with the magnitude of the change depending on the modeled configuration. The reported cooling-energy reduction is approximately 288.36 MWh/year (7.41%) for the JSM-195SP 30° case and 296.92 MWh/year (7.63%) for the JS-190W-Special 30° case. These values represent differences in the annual simulation outputs. Their interpretation is linked to the thermal and shading assumptions represented in the building-energy model and does not independently establish a specific heat-transfer mechanism beyond the modeled conditions.

Carbon-footprint screening used the 2026 EIB Project Carbon Footprint Methodologies factor for Egypt: 498 gCO_2/kWh for the combined margin associated with intermittent generation, including solar. The baseline footprint is 572.52 tCO_2/year, based on modeled grid electricity of 1,149,629.45 kWh/year. Applying net grid reductions yields post-PV footprints of 520.88, 540.32, 464.12, and 502.50 tCO_2/year for JSM-195SP and JS-190W-Special at 90° and 30°, respectively. Corresponding avoided emissions are 51.63, 32.20, 108.40, and 70.02 tCO_2/year. Each tonne of verified, eligible reduction could represent one carbon-credit unit; however, modeled reductions are not automatically certified or monetizable without an applicable standard, registration, additionality assessment, monitoring, reporting, verification, and ownership/retirement arrangements.

Table 12. Panels impact

Indicator	Baseline	JSM-195SP @ 30°	JS-190W-Special @ 30°
District cooling (kWh/yr)	3,893,520.27	3,605,158.05	3,596,599.31
Cooling change	—	−288,362.22 (−7.41%)	−296,920.96 (−7.63%)
District heating (kWh/yr)	104,393.77	64,828.53	65,198.53
Occupied cooling setpoint not met (h)	21.50	23.50	22.50
ASHRAE 55 simple comfort: not comfortable (h)	1,619.50	1,289.00	1,257.00

4.5.1. Carbon footprint and avoided operational emissions

Gross PV generation and purchased-grid reductions are accounted for separately. Gross PV generation corresponds to avoided emissions of 54.35, 33.89, 114.10, and 73.70 tCO_2/year for JSM-195SP and JS-190W-Special at 90° and 30°, respectively. Based on net grid-electricity reductions, the values are 51.63, 32.20, 108.40, and 70.02 tCO_2/year. The latter are used for carbon-credit screening because they align with the modeled net grid reduction and building electricity boundary.

Carbon-footprint assessment was performed using the 2026 European Investment Bank (EIB) Project Carbon Footprint Methodologies, Version 11.4. For Egypt, the methodology reports an emission factor of 498 gCO_2/kWh for the combined margin associated with intermittent electricity generation, which applies to solar PV generation. Accordingly, the annual avoided operational emissions attributable to the modeled PV generation were calculated as: Avoided CO_2 = annual PV generation × 0.498 $kgCO_2$/kWh.

Annual avoided operational CO_2 emissions were estimated using a grid-emission factor of 0.498 $kgCO_2$/kWh and each scenario's net grid-electricity reduction relative to baseline. This links emission reductions to avoided grid purchases rather than assuming gross PV generation directly equals avoided emissions. The results represent estimated operational reductions under the study's accounting assumptions.

Carbon-credit valuation is an illustrative scenario based on an assumed credit price, not confirmed revenue. Avoided emissions alone do not establish eligibility for credit issuance or sale; therefore, potential monetary value is treated separately from physical emission reductions and not as guaranteed income.

The baseline purchased-grid-electricity footprint was separately estimated from the DesignBuilder annual grid-electricity value of 1,149,629.45 kWh/year, giving 572.52 tCO_2/year. This distinction is maintained because gross PV generation and the simulated net grid reduction represent different accounting quantities. The resulting avoided-emission comparison is shown in **Figure 19, while Figure 20** presents the corresponding baseline and post-PV operational grid-electricity footprints.

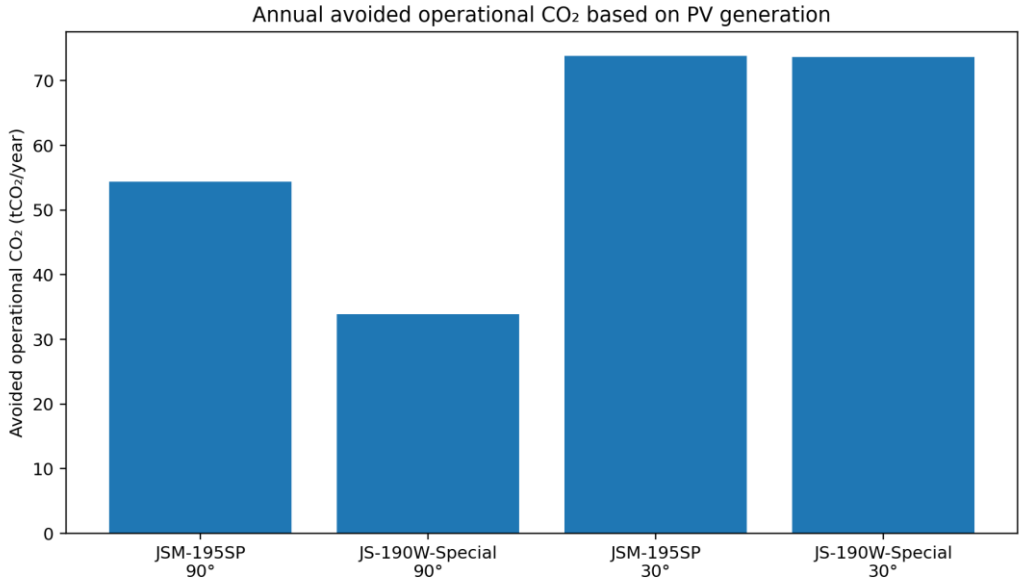

Figure 19. Annual avoided operational CO_2 associated with modeled PV generation.

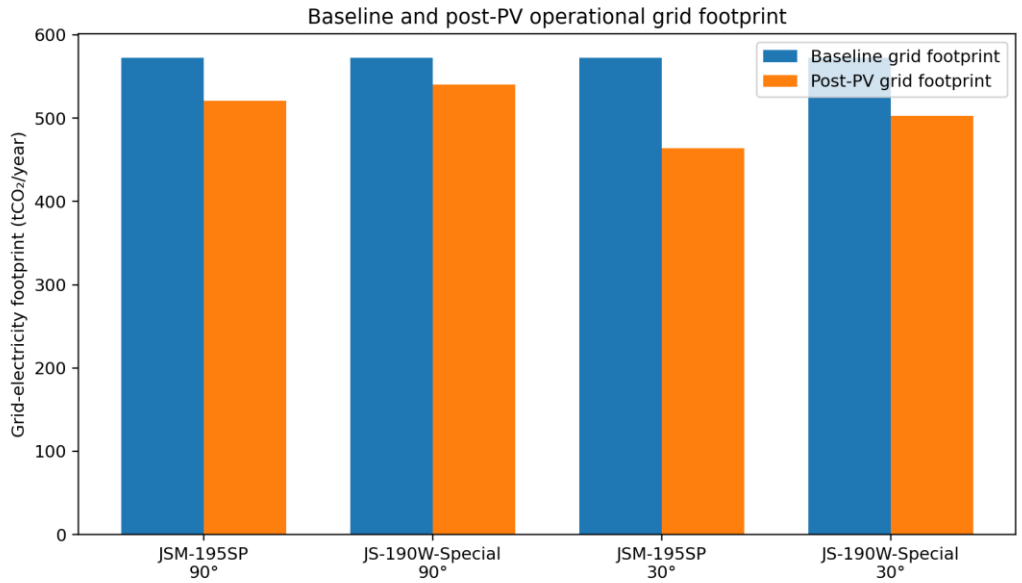

Figure 20. Baseline versus post-PV operational grid-electricity footprint.

4.6. Integrated electrical-energy comparison

Table 13 presents the carbon-footprint and potential carbon-credit screening based on modeled net grid reduction, while the configuration of panels is presented in **Table 14**.

Table 13. Carbon-footprint and potential carbon-credit screening based on modeled net grid reduction.

Scenario	Net grid reduction (kWh/yr)	Baseline footprint (tCO_2/yr)	Post-PV footprint (tCO_2/yr)	Avoided emissions (tCO_2/yr)	Potential credit quantity (tCO_2e/yr)	Illustrative VCM value (USD/yr)
Baseline	0.00	572.52	572.52	0.00	0.00	0.00
JSM-195SP @ 90°	103,676.19	572.52	520.88	51.63	51.63	293.78
JS-190W-Special @ 90°	64,651.41	572.52	540.32	32.20	32.20	183.20
JSM-195SP @ 30°	217,663.62	572.52	464.12	108.40	108.40	616.78
JS-190W-Special @ 30°	140,595.18	572.52	502.50	70.02	70.02	398.39

Note: 0.498 kgCO_2/kWh is the EIB 2026 Egypt combined-margin factor for intermittent electricity generation. The illustrative carbon-credit value uses USD 5.69/tCO_2e, the Q1 2026 average retirement price reported by Sylvera; it is a market-value illustration, not a guaranteed revenue or proof of credit eligibility.

Table 14. Configuration of panels

Configuration	July (kWh)	August (kWh)	July + August (kWh)	Mean POA July (W/m²)	Mean POA August (W/m²)
JSM-195SP 90°	18.51	7.66	26.17	151.94	162.45
JSM-195SP 30°	38.96	15.19	54.15	323.91	325.92
JS-190W-Special 90°	38.80	16.09	54.89	151.94	162.45
JS-190W-Special 30°	57.70	21.69	79.39	323.91	325.92

The techno-economic comparison was updated to use the practical panel counts required for 100% of the adopted annual Building Electricity reference. The corresponding module-only CAPEX values are therefore 3.762 million EGP for JSM-195SP at 90°, 29.016 million EGP for JS-190W-Special at 90°, 1.794 million EGP for JSM-195SP at 30°, and 13.344 million EGP for JS-190W-Special at 30°. These values are module purchase allowances rather than complete installed-system quotations; inverter, mounting/substructure, wiring, protection, installation, maintenance, replacement, and other balance-of-system costs are excluded.

4.7. Techno-economic performance

Under the revised 100% Building Electricity sizing, each configuration is scaled to the practical whole-panel count derived from the modeled annual panel productivity. JSM-195SP at 90° requires 627 panels; JS-190W-Special at 90° requires 2,418 panels; JSM-195SP at 30° requires 299 panels; and JS-190W-Special at 30° requires 1,112 panels. The corresponding module-only simple paybacks are 13.03, 100.55, 6.20, and 46.24 years, respectively, using the institutional tariff of 1.95 EGP/kWh. The 30° JSM-195SP configuration is therefore the most favorable option in the module-cost screening. The economic assessment distinguishes between module-only simple payback and the separate lifecycle evaluation. Module-only simple payback is based on the number of modules required for the selected electricity-generation target, the corresponding module purchase cost, and the annual electricity value adopted for that calculation. The lifecycle evaluation uses a broader set of financial assumptions, including the analysis period, discount rate, degradation, and operation and maintenance costs. Because these assessments use different cost boundaries and cash-flow assumptions, their resulting indicators describe different economic perspectives and are

interpreted separately. The revised economic analysis screens module costs for practical 100% Building Electricity sizing. Panel requirements are based on simulated configuration-specific productivity rather than fixed counts, identifying the minimum practical quantity needed to meet the annual target and enabling direct cost and payback comparisons. Investment-grade assessment requires verified installed CAPEX, inverter and balance-of-system costs, maintenance, replacement, financing, and applicable electricity-export/net-metering arrangements **Figures 21 and 22**.

4.7.1. Lifecycle techno-economic screening

A second, project-level screening is retained to distinguish module-only payback from a common installed-cost allowance. A screening CAPEX of approximately 3.63 million EGP is applied consistently to the four simulated façade configurations, together with the institutional tariff of 1.95 EGP/kWh, 0.7% annual PV degradation, 1.2% annual O&M, a 25-year analysis period, and a 10% discount rate **Table 15**. This CAPEX is an area-based screening allowance rather than a verified EPC quotation. Gross annual savings are calculated from modeled net grid reduction × tariff, while lifecycle indicators include O&M, degradation, discounting, IRR, NPV, discounted payback, and LCOE.

Table 15. Lifecycle economic comparison under the common 3.63 million EGP screening CAPEX and updated 1.95 EGP/kWh tariff.

Scenario	Grid reduction (kWh/yr)	Gross annual saving (EGP/yr)	Screening payback (yr)	Lifecycle payback after O&M (yr)	IRR	NPV @10% (EGP million)	Discounted payback (yr)	LCOE (EGP/kWh)
JSM-195SP @ 90°	103,676.19	202,169	17.96	22.89	−0.15%	−2.28	—	4.50
JS-190W-Special @ 90°	64,651.41	126,070	28.79	43.99	−4.94%	−2.94	—	7.22
JSM-195SP @ 30°	217,663.62	424,444	8.55	9.53	8.62%	−0.37	—	2.14
JS-190W-Special @ 30°	140,595.18	274,161	13.24	15.74	3.13%	−1.66	—	3.32

JSM-195SP at 30° remains the strongest lifecycle case. It gives approximately 424,444 EGP/year of gross electricity-cost savings, an 8.55-year screening payback, 8.62% IRR, and an NPV of approximately −0.37 million EGP at a 10% discount rate. Thus, it is technically and economically the best of the four cases under the adopted screening assumptions, but its lifecycle return remains below the 10% hurdle, and discounted payback is not achieved within 25 years.

4.8. Tariff-escalation sensitivity

The base-case lifecycle result is sensitive to future electricity-price escalation. The sensitivity below applies the stated annual tariff escalation to the electricity value stream while retaining the same 3.63 million EGP initial CAPEX, 0.7% PV degradation, 1.2% O&M, 25-year lifetime, and 10% discount rate. At zero escalation, the IRR is approximately 8.62%; increasing tariff escalation progressively improves IRR and produces a finite discounted payback once the resulting cash flows recover the investment on a discounted basis **Table 16**. The economic sensitivity assessment considers the effects of electricity-tariff escalation, system lifetime, discount rate, operation and maintenance costs, and PV performance degradation on the estimated investment performance. The existing tariff-escalation analysis evaluates changes in the value of generated electricity, while the additional sensitivity cases examine the influence of the principal lifecycle assumptions. The JSM-195SP configuration at 30° is used as the reference case because it provides the most favorable economic performance among the evaluated configurations. Each parameter is varied independently while the remaining assumptions are held constant, allowing its individual influence on the lifecycle indicators to be assessed. The results are interpreted within the assumptions and cost boundaries of the study **Table 16**.

Table 16. Sensitivity of lifecycle economics to annual electricity-tariff escalation for JSM-195SP at 30°.

Annual tariff escalation	IRR	NPV @10% (EGP million)	Discounted payback (yr)
0%	8.62%	-0.37	—
5%	13.87%	1.43	15
10%	18.92%	4.85	11

Annual tariff escalation	IRR	NPV @10% (EGP million)	Discounted payback (yr)
12%	20.91%	7.02	10
14%	22.89%	9.88	9
16%	24.86%	13.69	9
18%	26.82%	18.77	8
20%	28.77%	25.57	8

Table 17. Final façade-constrained PV sizing and module-cost simple-payback comparison.

Scenario	100% module count	Module price (EGP/panel)	Module-only CAPEX (EGP)	Scaled PV generation (kWh/yr)	Building Electricity coverage	Annual electricity value (EGP/yr)	Simple payback (yr)
JSM-195SP @ 90°	627	6,000	3,762,000	148,108.84	100.13%	288,812.24	13.03
JS-190W-Special @ 90°	2,418	12,000	29,016,000	147,980.99	100.04%	288,562.93	100.55
JSM-195SP @ 30°	299	6,000	1,794,000	148,283.03	100.25%	289,151.91	6.20
JS-190W-Special @ 30°	1,112	12,000	13,344,000	147,994.92	100.05%	288,590.09	46.24

Note: The practical panel counts are proportional sizing estimates derived from the completed annual simulations and are not additional DesignBuilder runs. Scaled PV generation = modeled annual PV generation × (practical 100% panel count / modeled panel count). Annual electricity value = scaled PV generation × 1.95 EGP/kWh. Simple payback = module-only CAPEX ÷ annual electricity value.
Note: Annual avoided electricity cost = net grid reduction × 1.95 EGP/kWh. Simple payback = module-only CAPEX ÷ annual avoided electricity-cost value. Balance-of-system and installation costs are excluded.

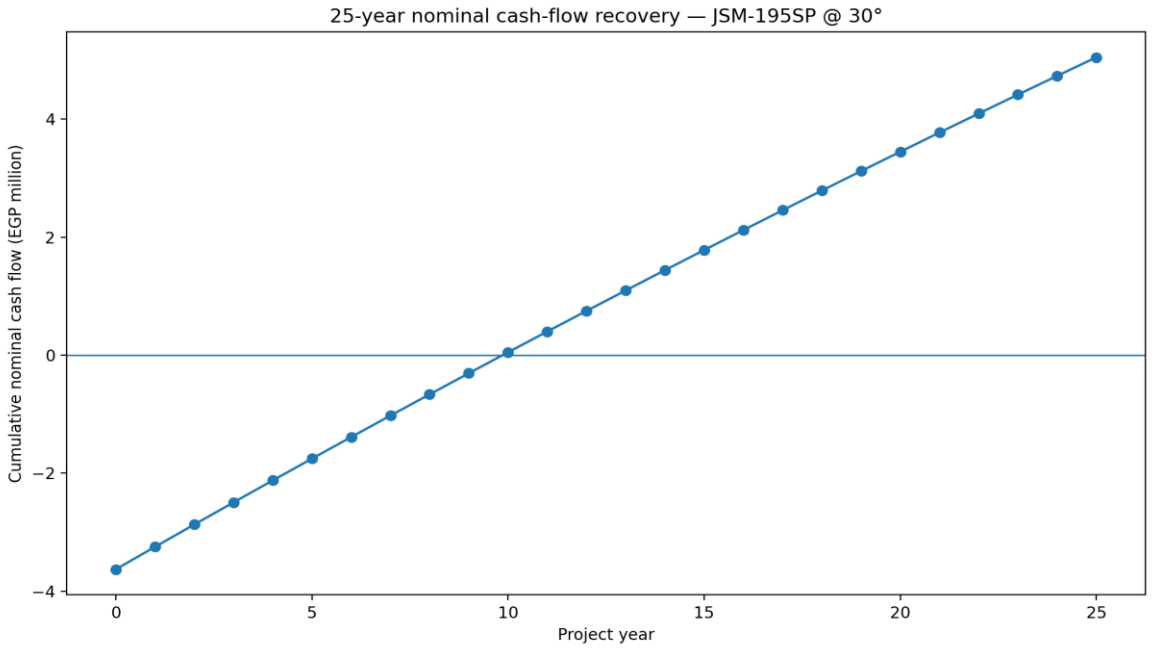

Figure 21. Cash-Flow recovery of selected panels.

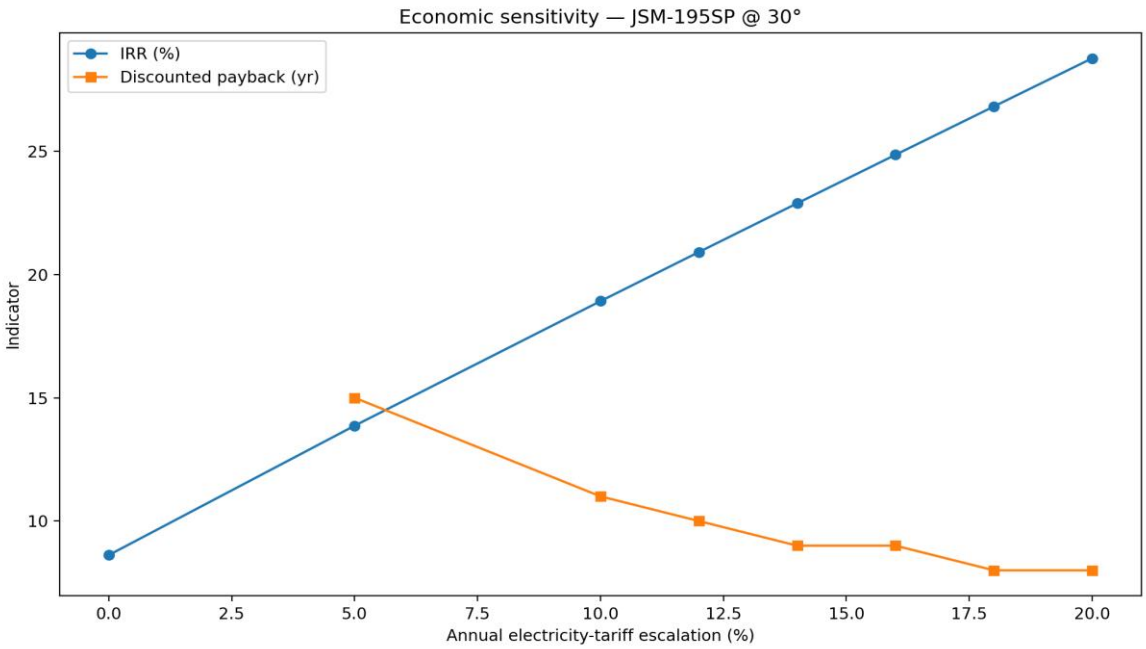

Figure 22. Economic sensitivity of Selected Panel.

4.9. Uncertainty and practical feasibility

Table 18. JSM-195SP @ 30 degree simple payback

Sensitivity case	Annual net grid reduction	Grid reduction	Module-cost simple payback
Base JSM-195SP @ 30°	217,663.62 kWh	18.93%	6.53 yr
PV output −5%	206,780.44 kWh	17.99%	6.87 yr
PV output +5%	228,546.80 kWh	19.88%	6.22 yr
Building demand +5%*	217,663.62 kWh	18.03%	6.53 yr

**For the demand +5% case, the absolute PV/grid offset is held at the simulated value while the percentage grid reduction is recalculated against the increased baseline grid demand. The sensitivity is a screening exercise and does not change the modeled PV output.*

Table 18. presents the JSM-195SP @ 30 degree simple payback. The practical implementation also requires structural verification of the 30° mounting arrangement, façade attachment and wind loading, waterproofing, maintenance access, DC/AC protection, cable sizing, string configuration, inverter sizing, and confirmation of the exact manufacturer datasheet. Rear ventilation or a ventilated cavity should be evaluated because PV operating temperature can influence both power output and envelope heat transfer. Shading-prone zones should be treated using electrical string segmentation or module-level power electronics where appropriate.

5. CONCLUSION

H1 is supported by the field measurements. The measured current and power profiles exhibit the expected daylight-dependent response and provide a direct empirical reference for component behavior. The evidence is deliberately limited to electrical response and does not constitute annual building-model calibration.

H2 is strongly supported. Both the weather-adjusted time series and the annual DesignBuilder simulations show a substantial increase when the collector is changed from 90° to 30°. For JSM-195SP, annual PV generation increases by 109.99 MWh/year; for JS-190W-Special, the increase is 79.94 MWh/year.

H3 is supported at building scale. JSM-195SP at 30° reduces Net Site Energy from 5,145,735.60 to 4,650,493.68 kWh/year and reduces net grid electricity by 217,663.62 kWh/year, equivalent to 18.93% of the baseline grid demand. The building remains a net energy consumer, so the result is a reduction in grid dependence rather than proof of NZEB status.

H4 is supported by the façade-specific solar screening and the measured sensitivity to local electrical conditions. E01 is the strongest vertical façade, while the field and time-series results show that electrical performance depends strongly on solar incidence and inclination. The final design should therefore be selective and shading-aware rather than uniformly distributed.

H5 is supported by the revised module-cost economic screening. JSM-195SP at 30° combines the highest annual PV generation, largest net grid reduction, lowest Net EUI, largest avoided operational emissions, and the shortest module-cost simple payback among the four modeled cases.

The field measurements remain experimental supporting evidence rather than annual utility validation, and the July–August series is treated as weather-adjusted estimated data. The annual simulations use the supplied EGY ETMY weather file identified by WMO station number “624200 Beheira” rather than a weather file specific to Damanhour; this limitation introduces uncertainty into the site-specific interpretation of the simulated annual results.

. Future work should therefore prioritize site-specific weather data, annual utility-meter validation, detailed structural and waterproofing design for the 30° mounting arrangement, rear-cavity ventilation assessment, module/string-level shading and mismatch analysis, detailed EPC/BOS costing, and long-term monitoring of an implemented façade PV system.

The solar-radiation screening identifies E01 as the strongest vertical façade at 1,141.2 kWh/m²·year, while the roof remains the highest-radiation surface overall at 1,726.8 kWh/m²·year. E01 is selected because the study specifically evaluates façade-applied PV. Among the controlled annual cases, JSM-195SP at 30° generates 229,119.60 kWh/year, equivalent to 495.93 kWh/panel·year on the modeled 462-panel basis. Normalization gives a practical requirement of 299 panels to reach 100% of the adopted annual Building Electricity reference, corresponding to an estimated 726.92 m² equivalent PV area, a module-only CAPEX of 1.794 million EGP, and a simple payback of approximately 6.20 years.

The results demonstrate a reduction in modeled grid-electricity demand rather than achievement of a formally established nearly zero-energy building classification. The practical PV sizing exercise uses the annual Building Electricity reference as a specific end-use target, whereas whole-building performance is evaluated separately through the annual building-energy results. The findings therefore support the use of façade-applied photovoltaics as a strategy for reducing grid dependence, but the reported reductions do not, on their own, establish compliance with a nearly zero-energy building standard.

This study establishes an experimentally supported, simulation-based framework for evaluating façade-applied PV in the Faculty of Engineering, Damanhour University. The workflow connects direct field measurements, weather-adjusted electrical analysis, controlled 8,760-hour DesignBuilder/EnergyPlus simulations, panel-productivity normalization, and economic screening. The annual simulations compare JSM-195SP and JS-190W-Special under the original 90° façade condition and a 30° inclined configuration while retaining the same building geometry, façade allocation, weather boundary, and PV-system representation.

REFERENCES

[1] M.M. Ibrahim, M.A. William, A.M. Elharidi, A.A. Hanafy, M.J. Suarez-Lopez, Do solar green roofs contribute to SDGs, fostering energy efficiency and environmental conservation?, Renew. Energy Sustain. Dev. 10 (2024) 258. https://doi.org/10.21622/resd.2024.10.2.924.

[2] J.H. Wesseling, S. Lechtenböhmer, M. Åhman, L.J. Nilsson, E. Worrell, L. Coenen, The transition of energy intensive processing industries towards deep decarbonization: Characteristics and implications for future research, Renew. Sustain. Energy Rev. 79 (2017) 1303–1313. https://doi.org/10.1016/j.rser.2017.05.156.

[3] Y. Teng, M. Bai, X. Lin, J. Li, T. Zhang, S. Liu, S. An, L. Xu, P. Wang, S. Han, J. Zhu, J. Zhu, H. Xie, Multi-scale assessment of energy transition and emission patterns in industrial coastal regions, Fuel 406 (2026) 137069. https://doi.org/10.1016/j.fuel.2025.137069.

[4] M.A. Hamied, M.A. Saad, P. García-Regodeseves, J.C. Ríos-Fernández, A novel integrated approach to heat transfer enhancement using baffles and inner fins in helical coil heat exchangers, Case Stud. Therm. Eng. 77 (2026) 107529. https://doi.org/10.1016/j.csite.2025.107529.

[5] A.M. Maghrabi, J. Song, C.N. Markides, How can industrial heat decarbonisation be accelerated through energy efficiency?, Appl. Therm. Eng. 233 (2023) 121092. https://doi.org/10.1016/j.applthermaleng.2023.121092.

[6] N.A. Moharram, A.H. Konsowa, A.I. Shehata, W.M. El-Maghlany, Advances in zero liquid discharge multigeneration plants: A novel approach for integrated power generation, supercritical desalination, and salt production, Energy Convers. Manag. 307 (2024) 118352. https://doi.org/10.1016/j.enconman.2024.118352.

[7] M.M. Ibrahim, M.J. Suarez-Lopez, A.A. Hanafy, M.A. William, Optimizing NZEB performance: A review of design strategies and case studies, Results Eng. 25 (2025) 103950. https://doi.org/10.1016/j.rineng.2025.103950.

[8] H. Setiawan, Towards sustainable energy access: evaluating free online photovoltaic design tools in support of the SDGs, Renew. Energy Sustain. Dev. 12 (2026) 41. https://doi.org/10.21622/resd.2026.12.1.1757.

[9] H.M. Maghrabie, M.A. Abdelkareem, A.H. Al-Alami, M. Ramadan, E. Mushtaha, T. Wilberforce, A.G. Olabi, State-of-the-Art Technologies for Building-Integrated Photovoltaic Systems, Buildings 11 (2021) 383. https://doi.org/10.3390/buildings11090383.

[10] A. Faes, A. Virtuani, H. Quest, L. Maturi, A. Scognamiglio, A. Frontini, A. Schlueter, N. Martin-Chivelet, A. Reinders, C. Ballif, Building-integrated photovoltaics, Nat. Rev. Clean Technol. 1 (2025) 333–350. https://doi.org/10.1038/s44359-025-00059-9.

[11] C. Vassiliades, Optimizing energy efficiency in mediterranean single-family homes: A parametric study of building typology, orientation, and BIPV integration, Renew. Energy 237 (2024) 121541. https://doi.org/10.1016/j.renene.2024.121541.

[12] D.C. Jordan, C. Deline, M. Deceglie, T.J. Silverman, W. Luo, PV Degradation – Mounting and Temperature, 2019 IEEE 46th Photovoltaic Specialists Conference, IEEE, 2019, pp. 0673–0679. https://doi.org/10.1109/PVSC40753.2019.8980767.

[13] K.G. Gabrovska-Evstatieva, D.T. Trifonov, B.I. Evstatiev, A Review of the Key Factors Influencing the Performance of Photovoltaic Installations in an Urban Environment, Electricity 6 (2025) 23. https://doi.org/10.3390/electricity6020023.

[14] M. Abdelmagied Hamied, A. Mohamed El-Haridi, W. Mohamed El-Maghlany, A. Ahmed Hanafy, Improving Office Building Energy Performance Using Phase Change Material in Building Envelope, in: 11th Int. Conf. Informatics, Environ. Energy Appl., ACM, 2022, pp. 52–55. https://doi.org/10.1145/3533254.3533264.

[15] O. Irulegi, A. Ruiz-Pardo, A. Serra, J.M. Salmerón, R. Vega, Retrofit strategies towards Net Zero Energy Educational Buildings: A case study at the University of the Basque Country, Energy Build. 144 (2017) 387–400. https://doi.org/10.1016/j.enbuild.2017.03.030.

[16] M. Krarti, P. Ihm, Evaluation of net-zero energy residential buildings in the MENA region, Sustain. Cities Soc. 22 (2016) 116–125. https://doi.org/10.1016/j.scs.2016.02.007.

[17] S. Albadry, K. Tarabieh, H. Sewilam, Achieving Net Zero-Energy Buildings through Retrofitting Existing Residential Buildings Using PV Panels, Energy Procedia 115 (2017) 195–204. https://doi.org/10.1016/j.egypro.2017.05.018.

[18] S. Attia, A. Evrard, E. Gratia, Development of benchmark models for the Egyptian residential buildings sector, Appl. Energy 94 (2012) 270–284. https://doi.org/10.1016/j.apenergy.2012.01.065.

[19] H.S.M. Shahin, Adaptive building envelopes of multistory buildings as an example of high performance building skins, Alexandria Eng. J. 58 (2019) 345–352. https://doi.org/10.1016/j.aej.2018.11.013.

[20] S. Yang, A. Cannavale, A. Di Carlo, D. Prasad, A. Sproul, F. Fiorito, Performance assessment of BIPV/T double-skin façade for various climate zones in Australia: Effects on energy consumption, Sol. Energy 199 (2020) 377–399. https://doi.org/10.1016/j.solener.2020.02.044.

[21] S. Sarihi, F. Mehdizadeh Saradj, M. Faizi, A Critical Review of Façade Retrofit Measures for Minimizing Heating and Cooling Demand in Existing Buildings, Sustain. Cities Soc. 64 (2021) 102525. https://doi.org/10.1016/j.scs.2020.12.007.

[22] A. Dutta, A. Samanta, Reducing cooling load of buildings in the tropical climate through window glazing: A model to model comparison, J. Build. Eng. 15 (2018) 318–327. https://doi.org/10.1016/j.jobe.2017.12.005.

[23] A. Fathalian, H. Kargarsharifabad, Actual validation of energy simulation and investigation of energy management strategies (Case Study: An office building in Semnan, Iran), Case Stud. Therm. Eng. 12 (2018) 510–516. https://doi.org/10.1016/j.csite.2018.06.007.

[24] M.M. Ibrahim, M.A. William, A.A. Hanafy, M.F. Moussa, M.J. Suarez-Lopez, Multi-pronged strategies for enhancing building envelopes toward nearly-zero energy in hot climatic regions, Eng. Res. Express 6 (2024) 045532. https://doi.org/10.1088/2631-8695/ad898a.

[25] A. Buonomano, G. De Luca, U. Montanaro, A. Palombo, Innovative technologies for NZEBs: An energy and economic analysis tool and a case study of a non-residential building for the Mediterranean climate, Energy Build. 121 (2016) 318–343. https://doi.org/10.1016/j.enbuild.2015.08.037.

[26] S. Bayoumi, N.A. Moharram, A.I. Shehata, M.M. Imam, W.M. El-Maghlany, A multi-criteria performance assessment of concentrated solar power plants for site and technology selection in Egypt, Int. J. Environ. Sci. Technol. 21 (2024) 2989–3004. https://doi.org/10.1007/s13762-023-05114-1.

[27] BIPV | Jet-Solar, (n.d.). https://www.jet-solar.com/en/bipv (accessed May 3, 2026).

[28] M. Elmnifi, D.T. Aleksandrovna, A.F.A. Fadiel, A.I. Shehata, N.A. Moharram, A.A. Taha, Unlocking hybrid solar efficiency: Experimental integration of aluminum foam fins and nanofluids in PVT collectors, Results Eng. 29 (2026) 108751. https://doi.org/10.1016/j.rineng.2025.108751.

[29] M. El Hadi Attia, A. Khelifa, A.E. Kabeel, M. Fayed, W.M. El-Maghlany, N.A. Moharram, A novel PVT system integrated with semicircular fins: CFD-based analysis of heat dissipation and energy efficiency, Appl. Therm. Eng. 279 (2025) 127551. https://doi.org/10.1016/j.applthermaleng.2025.127551.

[30] M.A. William, M.J. Suárez-López, S. Soutullo, A.A. Hanafy, Techno-economic evaluation of building envelope solutions in hot arid climate: A case study of educational building, Energy Reports 7 (2021) 550–558. https://doi.org/10.1016/J.EGYR.2021.07.098.

[31] H. Gholami, H.N. Røstvik, D. Müller-Eie, Holistic economic analysis of building integrated photovoltaics (BIPV) system: Case studies evaluation, Energy Build. 203 (2019) 109461. https://doi.org/10.1016/j.enbuild.2019.109461.

[32] U. Nations, The 17 Goals | Sustainable Development, Department of Economic and Social Affairs (2023). https://sdgs.un.org/goals.

[33] A. Abdallah, M.A. William, N.A. Moharram, I.F. Zidane, Wake-resolved 3D CFD analysis of a J-blade vertical axis wind turbine: startup optimization and tip-speed trade-offs, Eng. Sci. Technol. an Int. J. 77 (2026) 102364. https://doi.org/10.1016/j.jestch.2026.102364.

[34] N.A. Moharram, A.H. Konsowa, A.I. Shehata, W.M. El-Maghlany, Sustainable seascapes: An in-depth analysis of multigeneration plants utilizing supercritical zero liquid discharge desalination and a combined cycle power plant, Alexandria Eng. J. 118 (2025) 523–542. https://doi.org/10.1016/j.aej.2025.01.091.

[35] S. Pless, P. Torcellini, Net-Zero Energy Buildings: A Classification System Based on Renewable Energy Supply Options, NREL/TP-550-44586, National Renewable Energy Laboratory, 2010. https://doi.org/10.2172/983417.

[36] Global Solar Atlas, (n.d.). https://globalsolaratlas.info/ (accessed May 3, 2026).

[37] Weather Alexandria - meteoblue, (n.d.). https://www.meteoblue.com/en/weather/week/alexandria_egypt_361058 (accessed May 3, 2026).

[38] J. Águila-León, C. Vargas-Salgado, D. Díaz-Bello, C. Montagud-Montalvá, Optimizing photovoltaic systems: A meta-optimization approach for improving MPPT controllers, Renew. Energy 230 (2024) 120892. https://doi.org/10.1016/j.renene.2024.120892.

[39] Q. Yu, S. Chan, K. Chen, B. Zhao, X. Ren, G. Pei, Numerical and experimental study of a novel vacuum photovoltaic/thermal collector for efficient solar energy harvesting, Appl. Therm. Eng. 236 (2024) 121580. https://doi.org/10.1016/j.applthermaleng.2023.121580.

[40] W.M. El-Maghlany, M.E.H. Attia, A.E. Kabeel, M.A. Elazab, A. Hidouri, N.A. Moharram, Comparative experimental study on the performance of single-slope, hemispherical, and conical solar stills, Arch. Thermodyn. (2025) 187–187. https://doi.org/10.24425/ather.2025.156590.

[41] W.S. Ebhota, P.Y. Tabakov, Influence of photovoltaic cell technologies and elevated temperature on photovoltaic system performance, Ain Shams Eng. J. 14 (2023) 101984. https://doi.org/10.1016/j.asej.2022.101984.

[42] J. Appelbaum, A. Peled, A. Aronescu, Shadow Analysis of Photovoltaic Systems Deployed Near Obscuring Walls, Energies 18 (2025) 4839. https://doi.org/10.3390/en18184839.

[43] H. Gholami, H. Nils Røstvik, N. Manoj Kumar, S.S. Chopra, Lifecycle cost analysis (LCCA) of tailor-made building integrated photovoltaics (BIPV) façade: Solsmaragden case study in Norway, Sol. Energy 211 (2020) 488–502. https://doi.org/10.1016/j.solener.2020.09.087.

[44] A. Perrelli, E. Sodré, V. Silva, A. Santos, Maximizing Returns and Minimizing Risks in Hybrid Renewable Energy Systems: A Stochastic Discounted Cash Flow Analysis of Wind and Photovoltaic Systems in Brazil, Energies 16 (2023) 6833. https://doi.org/10.3390/en16196833.

[45] N.A. Moharram, S. Bayoumi, A.A. Hanafy, W.M. El-Maghlany, Techno-economic analysis of a combined concentrated solar power and water desalination plant, Energy Convers. Manag. 228 (2021) 113629. https://doi.org/10.1016/j.enconman.2020.113629.

[46] IEA, Energy Efficiency 2023, International Energy Agency, Paris, 2023. https://www.iea.org/reports/energy-efficiency-2023.